

Memristor Circuits: Pulse Programming via Invariant Manifolds

Original

Memristor Circuits: Pulse Programming via Invariant Manifolds / Corinto, Fernando; Forti, Mauro. - In: IEEE TRANSACTIONS ON CIRCUITS AND SYSTEMS. I, REGULAR PAPERS. - ISSN 1549-8328. - 65:4(2018), pp. 1327-1339. [10.1109/TCSI.2017.2740999]

Availability:

This version is available at: 11583/2704464 since: 2018-03-27T10:54:57Z

Publisher:

Institute of Electrical and Electronics Engineers Inc.

Published

DOI:10.1109/TCSI.2017.2740999

Terms of use:

openAccess

This article is made available under terms and conditions as specified in the corresponding bibliographic description in the repository

Publisher copyright

IEEE postprint/Author's Accepted Manuscript

©2018 IEEE. Personal use of this material is permitted. Permission from IEEE must be obtained for all other uses, in any current or future media, including reprinting/republishing this material for advertising or promotional purposes, creating new collecting works, for resale or lists, or reuse of any copyrighted component of this work in other works.

(Article begins on next page)

Memristor Circuits: Pulse Programming via Invariant Manifolds

Fernando Corinto, *Senior Member, IEEE*, and Mauro Forti

Abstract—The paper considers a large class of memristor circuits of arbitrary order, and containing an arbitrary number of flux- or charge-controlled memristors, for which a state equation (SE) description can be obtained. By means of the SEs, it is shown that the state space of each circuit can be decomposed in infinitely many manifolds, and that in the *autonomous* case each manifold is positively invariant and is characterized by a different reduced-order dynamics and attractors. These results are the basis for extending the analysis to the *non-autonomous* case where time-varying independent sources are present. In particular, the chief result obtained in the paper shows how to *analytically design external pulses for programming memristor circuits*, i.e., how invariant manifolds and attractors can be changed and controlled by applying suitable charge or flux sources via time-varying voltage and/or current pulses with finite time duration. The main results are obtained by relying on a recently introduced technique for the analysis of memristor circuits in the flux-charge domain.

Index Terms—Memristor, circuit theory, nonlinear dynamics, bifurcations, invariant manifolds, coexisting attractors.

I. INTRODUCTION

RECENTLY, the authors have introduced in [1], [2] a new technique, named “Flux-Charge Analysis Method” (FCAM), for the analysis of a wide class of dynamic memristor circuits in the flux-charge (φ, q) -domain. FCAM is based on using Kirchhoff flux and charge laws, and constitutive relations of circuit elements, directly expressed in the (φ, q) -domain and, as such, it basically differs from other traditional approaches for analyzing memristor circuits described in the voltage-current (v, i) -domain [3]–[7]. Also worthy of mention are flux-charge models of actual memristor devices derived from experimental results [8], [9] and a complete classification of memristors in terms of flux and charge [10].

The application of FCAM to specific low-order autonomous memristor circuits has shown that the state space in the (v, i) -domain can be decomposed in infinitely many positively invariant manifolds and that on each manifold the circuit is characterized by a different reduced-order dynamics and attractors. An interesting consequence is that bifurcations may be induced in two different ways. In the classical way, where the circuit parameters are changed for initial conditions (ICs) belonging to a fixed manifold (standard bifurcations).

Otherwise, by changing invariant manifold due to different ICs for fixed circuit parameters (also known as bifurcations without parameters [2]). In particular, in [1], [2] FCAM is used to analyze the dynamics and saddle-node bifurcations due to varying ICs for the simplest memristor circuit composed by a capacitor and a flux-controlled memristor, and the Hopf and period-doubling bifurcations leading to chaotic behavior, induced once more by varying the ICs, for some memristor oscillatory circuits. In overall, the results in [1], [2] have provided an analytic explanation of intriguing dynamic phenomena displayed by memristor circuits, as the co-existence of several attractors for the same set of parameters, and the sensitivity to ICs of the long-term behavior of solutions. We stress that such phenomena have been previously investigated mainly via numerical, or experimental means, see, e.g., [11]–[19], and references therein.

In [1], [2], only specific low-order autonomous memristor circuits have been considered for which invariant manifolds, and the dynamics on manifolds, are obtained by writing by inspection the state equations (SEs) via FCAM and relying on ad hoc mathematical manipulations of these SEs. Due to the huge variety and complexity of memristor circuits encountered in different applications (e.g., memristor synapses for neuromorphic systems, memristor-based chaotic circuits for cryptography, memristor-based biosensors, etc.), it would be desirable to develop a technique to study the existence of invariant manifolds, to derive their explicit expression, and to obtain the reduced-order dynamics on invariant manifolds, that is applicable to a large class of memristor circuits used in the technical applications. The main results in the paper concerning this point are as follows:

- (a) we introduce a systematic method for writing the differential algebraic equations (DAEs) and the SEs, both in the (φ, q) and in the (v, i) -domain, of a general class of memristor circuits of any order and with any number of flux- or charge-controlled memristors;
- (b) in the *autonomous* case, under certain assumptions, we introduce a new systematic method to identify and write analytically the invariant manifolds and to obtain the reduced-order dynamics on each invariant manifold.

The results in (a) and (b) are then used and extended for addressing the *non-autonomous* case, i.e., the case where time-varying independent sources are present in the memristor circuit. In this regard the chief contribution is as follows:

- (c) we develop analytic results showing how invariant manifolds, reduced-order dynamics, and attractors of non-autonomous memristor circuits can be programmed (i.e., how solutions can be driven between different manifolds

Copyright (c) 2016 IEEE. Personal use of this material is permitted. However, permission to use this material for any other purposes must be obtained from the IEEE by sending an email to pubs-permissions@ieee.org.

The support from European Cooperation in Science and Technology “COST Action IC1401” is acknowledged.

F. Corinto is with the Department of Electronics and Telecommunications, Politecnico di Torino, Torino, Italy, e-mail: (fernando.corinto@polito.it).

M. Forti is with the Department of Information Engineering and Mathematics, University of Siena, v. Roma 56 - 53100 Siena, Italy, e-mail: (forti@diism.unisi.it).

and dynamics) by applying suitable charge and/or flux sources via time-varying current and/or voltage pulses with finite time duration.

II. NETWORK STRUCTURE AND DAE DESCRIPTION

Consider the class \mathcal{LM} of *memristor circuits* \mathcal{N} constituted by n_C ideal capacitors, n_L ideal inductors, n_R ideal resistors, n_E ideal independent voltage sources, n_A ideal independent current sources, and n_M memristors that are either flux-controlled or charge-controlled.¹ Assume that:

- flux-controlled memristors are described by $q(t) = f(\varphi(t))$, where $\varphi(t)$ and $q(t)$ are the flux and charge in the memristor (i.e., the voltage and current momenta [20]), respectively. The nonlinear function $f(\cdot)$ is of class \mathbb{C}^2 for any φ and there exist $\sigma < \infty$ and $\epsilon_0 > 0$ such that $f'(\varphi) > \epsilon_0$ for any $|\varphi| \geq \sigma$
- charge-controlled memristors are described by $\varphi(t) = h(q(t))$, where the nonlinear function $h(\cdot)$ has mathematical properties similar to $f(\cdot)$.

We wish to analyze the nonlinear dynamics and bifurcations in memristor networks \mathcal{N} for $t \geq t_0$, where t_0 is a given finite time instant. For any two-terminal circuit element in \mathcal{N} , in addition to the voltage $v(t)$, current $i(t)$, flux $\varphi(t)$ and charge $q(t)$, we consider also the *incremental* flux and charge

$$\varphi(t; t_0) = \varphi(t) - \varphi(t_0) = \int_{t_0}^t v(\tau) d\tau \quad (1a)$$

$$q(t; t_0) = q(t) - q(t_0) = \int_{t_0}^t i(\tau) d\tau \quad (1b)$$

and thus the following properties hold (the dot denotes the time derivative): $\varphi(t) = \varphi(t; t_0) + \varphi(t_0)$; $q(t) = q(t; t_0) + q(t_0)$; $\varphi(t_0; t_0) = 0$; $q(t_0; t_0) = 0$; $\dot{\varphi}(t; t_0) = \dot{\varphi}(t) = v(t)$; $\dot{q}(t; t_0) = \dot{q}(t) = i(t)$; $\dot{\varphi}(t_0; t_0) = \dot{\varphi}(t_0) = v(t_0)$; $\dot{q}(t_0; t_0) = \dot{q}(t_0) = i(t_0)$.

Hereinafter, \mathcal{N} is described by means of FCAM in the (φ, q) -domain (see [1] for constitutive relations (CRs) of circuits elements and topological constraints given by the Kirchhoff Flux Law (K φ L) and Kirchhoff Charge Law (K q L) in terms of incremental fluxes and charges).

Goal of the manuscript is first to obtain via FCAM a DAE description of the networks \mathcal{N} in \mathcal{LM} and, on this basis, and under suitable assumptions, to obtain the explicit SEs for a large subclass of memristor networks \mathcal{N} in \mathcal{LM} . We stress that the knowledge of the SEs is a fundamental pre-requisite for studying basic qualitative aspects such as identifying the invariant manifolds and the dynamics on manifolds and study how dynamics through different manifolds can be controlled by external inputs. The importance to derive the explicit SEs for any dynamic network is clearly discussed in [21], [22] where one chief observation is that network models that do not admit a SE representation may be ill defined due to the presence of singular points (a.k.a. impasse points) where solutions cannot be continued.

To obtain a DAE description we note that, without losing generality, any $\mathcal{N} \in \mathcal{LM}$ can be decomposed into the

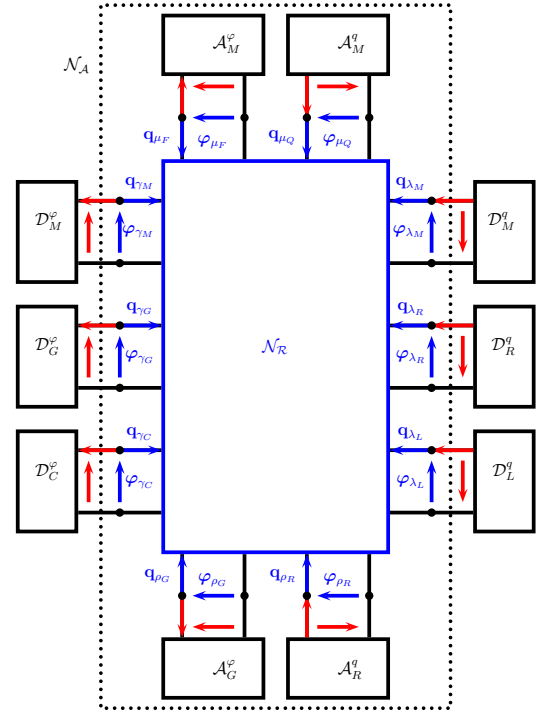


Figure 1: Decomposition of \mathcal{N} into \mathcal{N}_A and \mathcal{N}_D . The network $\mathcal{N}_D = \mathcal{D}^\varphi \cup \mathcal{D}^q$ contains all two-terminal elements external to \mathcal{N}_A . The n_C elements \mathcal{D}^φ , n_L elements \mathcal{D}^q and the linear network \mathcal{N}_R are highlighted. Reference directions for circuit elements external to \mathcal{N}_R are in red.

algebraic and the dynamic parts (see [21] for definition of algebraic and dynamics elements). In particular, \mathcal{N}_A denotes the nonlinear algebraic $(n_C + n_L)$ -ports with no capacitors and inductors, whereas \mathcal{N}_D (i.e., $\mathcal{N}_A \cup \mathcal{N}_D$ results to be \mathcal{N}) is assumed to be composed by n_C (resp., n_L) nonlinear dynamic flux-controlled (resp., charge-controlled) two-terminal elements \mathcal{D}^φ (resp., \mathcal{D}^q) connected to the ports of \mathcal{N}_A .² The conceptual decomposition of \mathcal{N} into \mathcal{N}_A and \mathcal{N}_D is shown in Fig. 1. We will see that the knowledge of the structure of \mathcal{N}_A is essential to develop a general methodology to study DAEs and SEs. In this regard, it is convenient to further decompose \mathcal{N}_A , i.e., to extract from \mathcal{N}_A the linear negative resistors and the memristors. Note that such negative resistors and memristors are not in parallel to a capacitor or in series with an inductor. Hence, \mathcal{N}_R is composed of positive resistors and/or independent sources (see again Fig. 1).

A. CRs of Two-terminal Elements

Here, we provide a systematic description of the different types of two-terminal elements in \mathcal{N}_D , \mathcal{N}_A and \mathcal{N}_R . For each two-terminal element connected to \mathcal{N}_R we use coordinated reference directions for incremental flux and charge as in [21, Fig. 20]. By [21, Theorem 2], the following cases can take place for any element \mathcal{D}^φ and \mathcal{D}^q in \mathcal{N}_D .³

²Mutual coupling between the elements \mathcal{D}^φ (and elements \mathcal{D}^q) is excluded since by assumption \mathcal{LM} is constituted of two-terminal elements, only.

³A negative resistor in parallel with a flux-controlled memristor or in series with a charge-controlled memristor can be embedded in any memristor in \mathcal{N} without modifying the results provided in this manuscript.

¹Resistors, capacitors and inductors can be either passive or active.

- γ_M is the number of $\mathcal{D}_M^\varphi \in \mathcal{N}_D$ made of a capacitor in parallel with a flux-controlled memristor; (incremental) fluxes and charges of \mathcal{D}_M^φ define the vectors $\varphi_{\gamma_M}(t; t_0)$ and $\mathbf{q}_{\gamma_M}(t; t_0)$, respectively. By FCAM [1], the CRs of \mathcal{D}_M^φ are expressed in the following vector form:⁴

$$\begin{aligned} -\mathbf{q}_{\gamma_M}(t; t_0) &= \mathbf{C}_{\gamma_M} \dot{\varphi}_{\gamma_M}(t; t_0) - \mathbf{q}_{C_{\gamma_M}}(t_0) \\ &+ f(\varphi_{\gamma_M}(t; t_0) + \varphi_{M_{\gamma_M}}(t_0)) \\ &- f(\varphi_{M_{\gamma_M}}(t_0)) \end{aligned} \quad (2)$$

where \mathbf{C}_{γ_M} is a diagonal matrix having the capacitance of capacitors in \mathcal{D}_M^φ and $\mathbf{q}_{C_{\gamma_M}}(t_0)$ are their ICs, whereas $\varphi_{M_{\gamma_M}}(t_0)$ are the ICs of memristors in \mathcal{D}_M^φ . The memristor fluxes in \mathcal{D}_M^φ are $\varphi_{M_{\gamma_M}}(t) = \varphi_{\gamma_M}(t; t_0) + \varphi_{M_{\gamma_M}}(t_0)$ and the capacitor voltages are $\mathbf{v}_{C_{\gamma_M}}(t) = \dot{\varphi}_{\gamma_M}(t; t_0)$.

- γ_G is the number of $\mathcal{D}_G^\varphi \in \mathcal{N}_D$ made of a capacitor in parallel with a negative resistor; fluxes and charges in such \mathcal{D}_G^φ define the vectors $\varphi_{\gamma_G}(t; t_0)$ and $\mathbf{q}_{\gamma_G}(t; t_0)$, respectively. The CRs of the elements \mathcal{D}_G^φ are

$$-\mathbf{q}_{\gamma_G}(t; t_0) = \mathbf{C}_{\gamma_G} \dot{\varphi}_{\gamma_G}(t; t_0) - \mathbf{q}_{C_{\gamma_G}}(t_0) + \mathbf{G}_{\gamma_G} \varphi_{\gamma_G}(t; t_0) \quad (3)$$

where \mathbf{C}_{γ_G} is a diagonal matrix having the capacitance of capacitors in \mathcal{D}_G^φ and $\mathbf{q}_{C_{\gamma_G}}(t_0)$ are their ICs.

- $\gamma_C = n_C - \gamma_M - \gamma_G$ is the number of $\mathcal{D}_C^\varphi \in \mathcal{N}_D$ made of just a capacitor; fluxes and charges in such capacitors define the vectors $\varphi_{\gamma_C}(t; t_0)$ and $\mathbf{q}_{\gamma_C}(t; t_0)$, respectively. The CRs of the elements \mathcal{D}_C^φ are

$$-\mathbf{q}_{\gamma_C}(t; t_0) = \mathbf{C}_{\gamma_C} \dot{\varphi}_{\gamma_C}(t; t_0) - \mathbf{q}_{C_{\gamma_C}}(t_0) \quad (4)$$

where \mathbf{C}_{γ_C} is a diagonal matrix having the capacitance of capacitors in \mathcal{D}_C^φ and $\mathbf{q}_{C_{\gamma_C}}(t_0)$ are their ICs.

- $\mathcal{D}^\varphi = \mathcal{D}_M^\varphi \cup \mathcal{D}_G^\varphi \cup \mathcal{D}_C^\varphi$ and $n_C = \gamma_M + \gamma_G + \gamma_C$.

We can use dual notations for $\mathcal{D}_M^q \in \mathcal{N}_D$ as follows.

- λ_M is the number of $\mathcal{D}_M^q \in \mathcal{N}_D$ made of an inductor in series with a charge-controlled memristors. The CRs are

$$\begin{aligned} -\varphi_{\lambda_M}(t; t_0) &= \mathbf{L}_{\lambda_M} \dot{\mathbf{q}}_{\lambda_M}(t; t_0) - \varphi_{L_{\lambda_M}}(t_0) \\ &+ h(\mathbf{q}_{\lambda_M}(t; t_0) + \mathbf{q}_{M_{\lambda_M}}(t_0)) \\ &- h(\mathbf{q}_{M_{\lambda_M}}(t_0)) \end{aligned} \quad (5)$$

where $\varphi_{L_{\lambda_M}}(t_0)$ (resp., $\mathbf{q}_{M_{\lambda_M}}(t_0)$) are the ICs for inductors (resp., memristors) in \mathcal{D}_M^q . The memristor charges in \mathcal{D}_M^q are $\mathbf{q}_{M_{\lambda_M}}(t) = \mathbf{q}_{\lambda_M}(t; t_0) + \mathbf{q}_{M_{\lambda_M}}(t_0)$ and the inductor currents are $\mathbf{i}_{L_{\lambda_M}}(t) = \dot{\mathbf{q}}_{\lambda_M}(t; t_0)$.

- λ_R is the number of $\mathcal{D}_R^q \in \mathcal{N}_D$ made of an inductor in series with a negative resistor. The CRs are

$$-\varphi_{\lambda_R}(t; t_0) = \mathbf{L}_{\lambda_R} \dot{\mathbf{q}}_{\lambda_R}(t; t_0) - \varphi_{L_{\lambda_R}}(t_0) + \mathbf{R}_{\lambda_R} \mathbf{q}_{\lambda_R}(t; t_0) \quad (6)$$

where $\varphi_{L_{\lambda_R}}(t_0)$ are the ICs of inductors in \mathcal{D}_R^q .

- $\lambda_L = n_L - \lambda_M - \lambda_R$ is the number of $\mathcal{D}_L^q \in \mathcal{N}_D$ made of just an inductor. The CRs are

$$-\varphi_{\lambda_L}(t; t_0) = \mathbf{L}_{\lambda_L} \dot{\mathbf{q}}_{\lambda_L}(t; t_0) - \varphi_{L_{\lambda_L}}(t_0) \quad (7)$$

where $\varphi_{L_{\lambda_L}}(t_0)$ are the ICs of inductors in \mathcal{D}_L^q .

- $\mathcal{D}^q = \mathcal{D}_M^q \cup \mathcal{D}_R^q \cup \mathcal{D}_L^q$ and $n_L = \lambda_M + \lambda_R + \lambda_L$.

For what concern the structure of \mathcal{N}_A let us assume that:

- μ_F is the number of flux-controlled memristors $\mathcal{A}_M^\varphi \in \mathcal{N}_A$ with CRs

$$-\mathbf{q}_{\mu_F}(t; t_0) = f(\varphi_{\mu_F}(t; t_0) + \varphi_{M_{\mu_F}}(t_0)) - f(\varphi_{M_{\mu_F}}(t_0)) \quad (8)$$

where $\varphi_{M_{\mu_F}}(t_0)$ are the ICs of memristors in \mathcal{A}_M^φ .

- μ_Q is the number of charge-controlled memristors $\mathcal{A}_M^q \in \mathcal{N}_A$ with CRs

$$-\varphi_{\mu_Q}(t; t_0) = h(\mathbf{q}_{\mu_Q}(t; t_0) + \mathbf{q}_{M_{\mu_Q}}(t_0)) - h(\mathbf{q}_{M_{\mu_Q}}(t_0)) \quad (9)$$

where $\mathbf{q}_{M_{\mu_Q}}(t_0)$ are the ICs of memristors in \mathcal{A}_M^q .

- ρ_G is the number of negative conductances $\mathcal{A}_G^\varphi \in \mathcal{N}_A$ with CRs

$$-\mathbf{q}_{\rho_G}(t; t_0) = \mathbf{G}_{\rho_G} \varphi_{\rho_G}(t; t_0) \quad (10)$$

- ρ_R is the number of negative resistors $\mathcal{A}_R^q \in \mathcal{N}_A$ with CRs

$$-\varphi_{\rho_R}(t; t_0) = \mathbf{R}_{\rho_R} \mathbf{q}_{\rho_R}(t; t_0) \quad (11)$$

Note that $n_M = \mu_F + \mu_Q + \gamma_M + \lambda_M$ is the total number of memristor in \mathcal{N} .

The extraction of \mathcal{A}_M^φ , \mathcal{A}_G^φ , \mathcal{A}_M^q and \mathcal{A}_R^q from \mathcal{N}_A produces a linear network \mathcal{N}_R with $(n_C + n_L + \mu_F + \mu_Q + \rho_G + \rho_R)$ ports having only positive (linear) resistors and independent sources. We have

- n_E ideal independent voltage sources $\mathbf{e}(t)$ such that $\varphi_e(t; t_0) = \int_{t_0}^t \mathbf{e}(\tau) d\tau$
- n_A ideal independent current sources $\mathbf{a}(t)$ such that $\mathbf{q}_a(t; t_0) = \int_{t_0}^t \mathbf{a}(\tau) d\tau$.

B. Hybrid Representation of \mathcal{N}_R

Among the different representations of the network \mathcal{N}_R , it is convenient to exploit its description in terms of a suitable hybrid matrix

$$\begin{pmatrix} \mathbf{q}_{\gamma_M}(t; t_0) \\ \varphi_{\lambda_M}(t; t_0) \\ \mathbf{q}_{\gamma_G}(t; t_0) \\ \varphi_{\lambda_R}(t; t_0) \\ \mathbf{q}_{\gamma_C}(t; t_0) \\ \varphi_{\lambda_L}(t; t_0) \\ \varphi_{\mu_Q}(t; t_0) \\ \mathbf{q}_{\mu_F}(t; t_0) \\ \varphi_{\rho_R}(t; t_0) \\ \mathbf{q}_{\rho_G}(t; t_0) \end{pmatrix} = \mathbf{H}_R \begin{pmatrix} \varphi_{\gamma_M}(t; t_0) \\ \mathbf{q}_{\lambda_M}(t; t_0) \\ \varphi_{\gamma_G}(t; t_0) \\ \mathbf{q}_{\lambda_R}(t; t_0) \\ \varphi_{\gamma_C}(t; t_0) \\ \mathbf{q}_{\lambda_L}(t; t_0) \\ \mathbf{q}_{\mu_Q}(t; t_0) \\ \varphi_{\mu_F}(t; t_0) \\ \mathbf{q}_{\rho_R}(t; t_0) \\ \varphi_{\rho_G}(t; t_0) \end{pmatrix} + \mathbf{u}(t; t_0) \quad (12)$$

where

- $\mathbf{u}(t; t_0)$ takes into account the effects due to the sources $\varphi_e(t; t_0)$ and $\mathbf{q}_a(t; t_0)$ within \mathcal{N}_R
- the independent port variables in \mathcal{N}_R are the fluxes in the two-terminal flux-controlled elements \mathcal{D}^φ , \mathcal{A}_M^φ and \mathcal{A}_G^φ and the charges in the two-terminal charge-controlled elements \mathcal{D}^q , \mathcal{A}_M^q and \mathcal{A}_R^q
- the dependent port variables in \mathcal{N}_R are the charges in the two-terminal flux-controlled elements and fluxes in the two-terminal charge-controlled elements.

⁴The source sign convention is used for any element \mathcal{D}^φ and \mathcal{D}^q in \mathcal{N}_D .

According to known properties of connected linear graphs [23]⁵, see also [24, Theorem 1], the hybrid description (12) of \mathcal{N}_R holds if and only if the following assumption (hereinafter named *Assumption 1*, or (A1) for short) holds

(A1) The subnetwork \mathcal{N}_R of \mathcal{N} satisfies the following topological constraints:

- there exist no loops made of the flux-controlled two-terminal elements \mathcal{D}^φ , \mathcal{A}_M^φ and \mathcal{A}_G^φ and/or the flux sources $\varphi_e(t; t_0)$ within \mathcal{N}_R
- there exist no cutsets made of the charge-controlled elements \mathcal{D}^q , \mathcal{A}_M^q and \mathcal{A}_R^q and/or the charge sources $q_a(t; t_0)$ within \mathcal{N}_R .

Remark 1: As reported in [24], the description of \mathcal{N}_R by means of the hybrid matrix \mathbf{H}_R is as general as the approach based on the incidence matrix and the Tableau method.

C. DAEs of \mathcal{N} in the (φ, q) -domain

The set of equations from (2) to (12) describe any memristor circuit $\mathcal{N} \in \mathcal{LM}$ that satisfies (A1) in terms of a system of DAEs in the (φ, q) -domain.

The next example shows that the derivation of the SEs from the DAEs require further assumptions on the memristor circuit \mathcal{N} . In particular, it shows that two-terminal elements in $\mathcal{N}_A \setminus \mathcal{N}_R$, such as negative resistors and/or charge-controlled memristors not in series with an inductor and, by duality, negative conductances and/or flux-controlled memristors not in parallel with a capacitor, might cause problems for the existence of the SE description.

Example: Consider the memristor circuit in Fig. 2 in the (φ, q) -domain, that is obtained from that in [2, Section II.A] by including a negative resistor ($R < 0$) and a linear two-terminal element \mathcal{N}_R represented by its Thevenin equivalent circuit made of the resistor $R_1 \geq 0$ and the flux source $\varphi_e(t; t_0)$. The DAE description in the (φ, q) -domain is

$$C\dot{\varphi}_C(t; t_0) = -q_M(t; t_0) + q_C(t_0) \quad (13a)$$

$$\begin{aligned} h(q_M(t)) + (R_1 + R)q_M(t) &= \varphi_C(t; t_0) - \varphi_e(t; t_0) \\ &\quad + h(q_M(t_0)) + (R_1 + R)q_M(t_0) \end{aligned} \quad (13b)$$

for $t \geq t_0$, where $q_C(t_0) = Cv_C(t_0)$, $q_M(t_0)$ are the ICs for the state variables in the (v, i) -domain. The explicit SE for the memristor circuit in Fig. 2 can be derived from the DAE (13) only under suitable assumptions on the negative resistor R and the nonlinearity of the charge-controlled memristor.

In particular, the following cases can take place:

- 1) if $R = -R_1$ and $h(\cdot)$ is monotone, hence $q_M(t) = h^{-1}(\varphi_C(t; t_0) - \varphi_e(t; t_0) + h(q_M(t_0)))$, then the SE is
- $$C\dot{\varphi}_C(t; t_0) = -h^{-1}(\varphi_C(t; t_0) - \varphi_e(t; t_0) + h(q_M(t_0))) + q_C(t_0) + q_M(t_0). \quad (14)$$

On the contrary, if $R = -R_1$ but $\varphi_M(\cdot) = h(q_M(\cdot))$ is not monotone, then the DAE cannot be cast in the form of a SE. It can be seen that the memristor circuit in

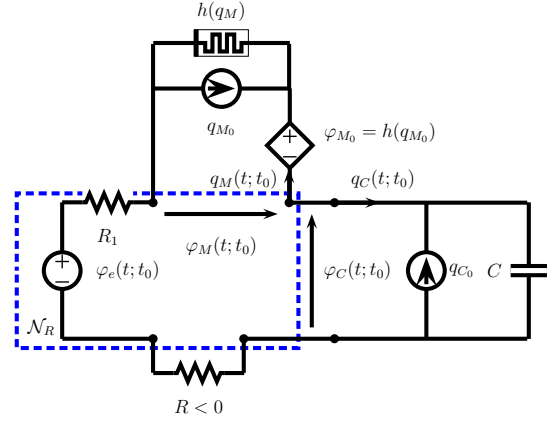


Figure 2: Example of decomposition of \mathcal{N} into \mathcal{N}_A and \mathcal{N}_D . The network \mathcal{N}_D contains only a capacitor. The network \mathcal{N}_A has a linear network \mathcal{N}_R , made up of a resistor $R_1 \geq 0$ and a flux source $\varphi_e(t; t_0)$, connected to a charge-controlled memristor $\varphi_M(\cdot) = h(q_M(\cdot))$ and a negative resistor $R < 0$.

Fig. 2 describes a *nonphysical situation* because it does not have a globally defined SE and it exhibits impasse points (see [2, Section II.A] for more details).

- 2) If $R \neq -R_1$ the DAE reduces to the next SE if and only if $H(q_M(t)) = h(q_M(t)) + (R_1 + R)q_M(t)$ is monotone

$$\begin{aligned} C\dot{\varphi}_C(t; t_0) &= -\mathcal{H}(\varphi_C(t; t_0), \varphi_e(t; t_0), q_M(t_0)) \\ &\quad + q_C(t_0) + q_M(t_0) \end{aligned} \quad (15)$$

where we have let $\mathcal{H}(\varphi_C(t; t_0), \varphi_e(t; t_0), q_M(t_0)) = H^{-1}(\varphi_C(t; t_0) - \varphi_e(t; t_0) + h(q_M(t_0)) + (R_1 + R)q_M(t_0))$. Note that, even if the memristor is passive, there are values of $R < 0$ for which the monotone condition on $H(q_M(t))$ fails, so that once more the SE does not exist and we have a nonphysical situation.⁶

III. SES OF \mathcal{N} IN THE (φ, q) -DOMAIN

We consider henceforth memristor circuits $\mathcal{N} \in \mathcal{LM}$ satisfying (A1). Consider also the following assumptions – denoted as *Assumption 2*, i.e., (A2), and *Assumption 3*, i.e., (A3) – enabling to specify all possible configurations of $\mathcal{N} = \mathcal{N}_D \cup \mathcal{N}_A$ according to the structure of \mathcal{N}_A :

- (A2) The subnetwork \mathcal{N}_A of \mathcal{N} has no memristors.
- (A3) The subnetwork \mathcal{N}_A of \mathcal{N} has no negative resistors.

Clearly, \mathcal{N} admits of only these four configurations:

- i) if both (A2) and (A3) are fulfilled then $\mu_F = \mu_Q = 0$ and $\rho_G = \rho_R = 0$, that is $\mathcal{N}_A = \mathcal{N}_R$ and $\mathcal{N} = \mathcal{N}_D \cup \mathcal{N}_R$
- ii) if only (A2) is fulfilled then $\mu_F = \mu_Q = 0$, $\rho_G \neq 0$ and $\rho_R \neq 0$, that is $\mathcal{N} = \mathcal{N}_D \cup \mathcal{N}_R \cup \mathcal{A}_G^\varphi \cup \mathcal{A}_R^q$
- iii) if only (A3) is fulfilled then $\mu_F \neq 0$, $\mu_Q \neq 0$ and $\rho_G = \rho_R = 0$, that is $\mathcal{N} = \mathcal{N}_D \cup \mathcal{N}_R \cup \mathcal{A}_M^\varphi \cup \mathcal{A}_M^q$

⁶In both cases $R = -R_1$ or $R \neq -R_1$, as shown in the example of [2, Sect II.A], a sufficient condition that always guarantees the explicit derivation of the SE for the memristor circuit in Fig. 2 is the introduction of an inductor in series with the charge-controlled memristor and the negative resistor.

⁵In particular, we can use the result described in the (v, i) -domain in [23, Section 7, p. 125], that can be extended *mutatis mutandis* to the (φ, q) -domain.

iv) if both (A2) and (A3) are not satisfied then $\mu_F \neq 0$, $\mu_Q \neq 0$, $\rho_G \neq 0$ and/or $\rho_R \neq 0$, that is $\mathcal{N} = \mathcal{N}_D \cup \mathcal{N}_R \cup \mathcal{A}_M^\varphi \cup \mathcal{A}_M^q \cup \mathcal{A}_G^\varphi \cup \mathcal{A}_R^q$.

The first case (i) is thoroughly investigated in this manuscript; the other cases can be discussed, *mutatis mutandis*, in a similar way. For the sake of brevity and the lack of space they will be reported in detail in a further work.

A. The Case $\mathcal{N} = \mathcal{N}_D \cup \mathcal{N}_R$

Suppose that (A1)-(A3) are satisfied, hence the memristor circuit \mathcal{N} is made of the $(n_C + n_L)$ -port \mathcal{N}_R connected to the n_C elements \mathcal{D}^φ and to the n_L elements \mathcal{D}^q . In this case (A1) is equivalent to the following assumption that can be easily checked by inspection: *the memristor network \mathcal{N} has no loops made by capacitors and/or flux sources and no cutsets made by inductors and/or charge sources.*

Moreover, the use of (2) to (12) directly yields the SE representation⁷ of \mathcal{N} in the (φ, q) -domain

$$\mathbf{M} \begin{pmatrix} \dot{\varphi}_{\gamma_M}(t; t_0) \\ \dot{\mathbf{q}}_{\lambda_M}(t; t_0) \\ \dot{\varphi}_{\gamma_G}(t; t_0) \\ \dot{\mathbf{q}}_{\lambda_R}(t; t_0) \\ \dot{\varphi}_{\gamma_C}(t; t_0) \\ \dot{\mathbf{q}}_{\lambda_L}(t; t_0) \end{pmatrix} = -(\mathbf{H}_R + \mathbf{G}) \begin{pmatrix} \varphi_{\gamma_M}(t; t_0) \\ \mathbf{q}_{\lambda_M}(t; t_0) \\ \varphi_{\gamma_G}(t; t_0) \\ \mathbf{q}_{\lambda_R}(t; t_0) \\ \varphi_{\gamma_C}(t; t_0) \\ \mathbf{q}_{\lambda_L}(t; t_0) \end{pmatrix} - \begin{pmatrix} f(\varphi_{\gamma_M}(t; t_0) + \varphi_{M_{\gamma_M}}(t_0)) \\ h(\mathbf{q}_{\lambda_M}(t; t_0) + \mathbf{q}_{M_{\lambda_M}}(t_0)) \\ \mathbf{0} \\ \mathbf{0} \\ \mathbf{0} \\ \mathbf{0} \end{pmatrix} + \begin{pmatrix} f(\varphi_{M_{\gamma_M}}(t_0)) \\ h(\mathbf{q}_{M_{\gamma_M}}(t_0)) \\ \mathbf{0} \\ \mathbf{0} \\ \mathbf{0} \\ \mathbf{0} \end{pmatrix} + \begin{pmatrix} \mathbf{q}_{C_{\gamma_M}}(t_0) \\ \varphi_{L_{\lambda_M}}(t_0) \\ \mathbf{q}_{C_{\gamma_G}}(t_0) \\ \varphi_{L_{\lambda_R}}(t_0) \\ \mathbf{q}_{C_{\gamma_C}}(t_0) \\ \varphi_{L_{\lambda_L}}(t_0) \end{pmatrix} + \mathbf{u}(t; t_0) \quad (16)$$

for $t \geq t_0$ where

- \mathbf{M} and \mathbf{G} are diagonal matrices defined as $\mathbf{M} = \text{diag}(\mathbf{C}_{\gamma_M}, \mathbf{L}_{\lambda_M}, \mathbf{C}_{\gamma_G}, \mathbf{L}_{\lambda_R}, \mathbf{C}_{\gamma_C}, \mathbf{L}_{\lambda_L})$ and $\mathbf{G} = \text{diag}(\mathbf{0}, \mathbf{0}, \mathbf{G}_{\gamma_G}, \mathbf{R}_{\lambda_R}, \mathbf{0}, \mathbf{0})$. In particular, \mathbf{M} is nonsingular;
- the state vector in the (φ, q) -domain includes the n_C fluxes across the capacitors (i.e., $\varphi_{\gamma_M}(t; t_0)$, $\varphi_{\gamma_G}(t; t_0)$ and $\varphi_{\gamma_C}(t; t_0)$) and n_L charges through the inductors (i.e., $\mathbf{q}_{\lambda_M}(t; t_0)$, $\mathbf{q}_{\lambda_R}(t; t_0)$ and $\mathbf{q}_{\lambda_L}(t; t_0)$);
- (16) is a system of $n = n_C + n_L$ ODEs in which the first $n_M = \gamma_M + \lambda_M$ ODEs are nonlinear, whereas the other $(n_C + n_L - n_M)$ ODEs are linear
- in general, the vector $\mathbf{u}(t, t_0)$ in (12) can be written in terms of the internal sources as

$$\mathbf{u}(t; t_0) = \mathbf{B} \begin{pmatrix} \varphi_e(t; t_0) \\ \mathbf{q}_a(t; t_0) \end{pmatrix}$$

⁷Strictly speaking, the SEs in the normal form are obtained by multiplying both sides of (16) by \mathbf{M}^{-1} .

with $\mathbf{B} \in \mathbb{R}^{(n_C + n_L) \times (n_E + n_A)}$.

It is useful to write the SEs in a more compact form by means of the following notations.

$$n_x = \gamma_M + \lambda_M = n_M \quad (17a)$$

$$n_y = (n_C + n_L) - n_x = n - n_x \quad (17b)$$

$$\mathbf{x}(t) = (\varphi_{\gamma_M}(t; t_0), \mathbf{q}_{\lambda_M}(t; t_0)) \in \mathbb{R}^{n_x} \quad (17c)$$

$$\mathbf{y}(t) = (\varphi_{\gamma_G}(t; t_0), \mathbf{q}_{\lambda_R}(t; t_0), \varphi_{\gamma_C}(t; t_0), \mathbf{q}_{\lambda_L}(t; t_0)) \in \mathbb{R}^{n_y} \quad (17d)$$

$$\mathbf{x}_M(t) = (\varphi_{M_{\gamma_M}}(t), \mathbf{q}_{M_{\lambda_M}}(t)) \in \mathbb{R}^{n_x} \quad (17e)$$

$$\mathbf{M}_x = \text{diag}(\mathbf{C}_{\gamma_M}, \mathbf{L}_{\lambda_M}) \in \mathbb{R}^{n_x \times n_x} \quad (17f)$$

$$\mathbf{M}_y = \text{diag}(\mathbf{C}_{\gamma_G}, \mathbf{L}_{\lambda_R}, \mathbf{C}_{\gamma_C}, \mathbf{L}_{\lambda_L}) \in \mathbb{R}^{n_y \times n_y} \quad (17g)$$

$$\mathbf{M} = \text{diag}(\mathbf{M}_x, \mathbf{M}_y) \in \mathbb{R}^{n \times n} \quad (17h)$$

$$\mathbf{F}(\cdot) = (f(\cdot), h(\cdot)) : \mathbb{R}^{n_x} \rightarrow \mathbb{R}^{n_x} \quad (17i)$$

$$\mathbf{u}(t; t_0) = \begin{pmatrix} \mathbf{u}_x(t) \\ \mathbf{u}_y(t) \end{pmatrix} = \begin{pmatrix} \mathbf{B}_{11} & \mathbf{B}_{12} \\ \mathbf{B}_{21} & \mathbf{B}_{22} \end{pmatrix} \begin{pmatrix} \varphi_e(t; t_0) \\ \mathbf{q}_a(t; t_0) \end{pmatrix} \quad (17j)$$

$$\mathbf{H} = \mathbf{H}_R + \mathbf{G} = \begin{pmatrix} \mathbf{H}_{11} & \mathbf{H}_{12} \\ \mathbf{H}_{21} & \mathbf{H}_{22} \end{pmatrix} \quad (17k)$$

where $\mathbf{H}_{11} \in \mathbb{R}^{n_x \times n_x}$, $\mathbf{H}_{12} \in \mathbb{R}^{n_x \times n_y}$, $\mathbf{H}_{21} \in \mathbb{R}^{n_y \times n_x}$ and $\mathbf{H}_{22} \in \mathbb{R}^{n_y \times n_y}$, whereas $\mathbf{B}_{11} \in \mathbb{R}^{n_x \times n_E}$, $\mathbf{B}_{12} \in \mathbb{R}^{n_x \times n_A}$, $\mathbf{B}_{21} \in \mathbb{R}^{n_y \times n_E}$ and $\mathbf{B}_{22} \in \mathbb{R}^{n_y \times n_A}$.

Note that $\mathbf{x}_M(t)$ is the state vector (fluxes and charges) of the memristors and we have

$$\mathbf{x}_M(t) = \mathbf{x}(t) + \mathbf{x}_M(t_0) \Rightarrow \dot{\mathbf{x}}_M(t) = \dot{\mathbf{x}}(t), \forall t \geq t_0. \quad (18)$$

In addition the following relationships hold for any $t \geq t_0$

$$\mathbf{M}_x \dot{\mathbf{x}}(t) = \mathbf{M}_x \begin{pmatrix} \mathbf{v}_{C_{\gamma_M}}(t) \\ \mathbf{i}_{L_{\lambda_M}}(t) \end{pmatrix} = \begin{pmatrix} \mathbf{q}_{C_{\gamma_M}}(t) \\ \varphi_{L_{\lambda_M}}(t) \end{pmatrix} \quad (19a)$$

$$\mathbf{M}_y \dot{\mathbf{y}}(t) = \mathbf{M}_y \begin{pmatrix} \mathbf{v}_{C_{\gamma_G}}(t) \\ \mathbf{i}_{L_{\lambda_R}}(t) \\ \mathbf{v}_{C_{\gamma_C}}(t) \\ \mathbf{i}_{L_{\lambda_L}}(t) \end{pmatrix} = \begin{pmatrix} \mathbf{q}_{C_{\gamma_G}}(t) \\ \varphi_{L_{\lambda_R}}(t) \\ \mathbf{q}_{C_{\gamma_C}}(t) \\ \varphi_{L_{\lambda_L}}(t) \end{pmatrix} \quad (19b)$$

$$\mathbf{M}_x \ddot{\mathbf{x}}(t) = \mathbf{M}_x \begin{pmatrix} \dot{\mathbf{v}}_{C_{\gamma_M}}(t) \\ \dot{\mathbf{i}}_{L_{\lambda_M}}(t) \end{pmatrix} = \begin{pmatrix} \dot{\mathbf{q}}_{C_{\gamma_M}}(t) \\ \mathbf{v}_{L_{\lambda_M}}(t) \end{pmatrix} \quad (19c)$$

$$\mathbf{M}_y \ddot{\mathbf{y}}(t) = \mathbf{M}_y \begin{pmatrix} \dot{\mathbf{v}}_{C_{\gamma_G}}(t) \\ \dot{\mathbf{i}}_{L_{\lambda_R}}(t) \\ \dot{\mathbf{v}}_{C_{\gamma_C}}(t) \\ \dot{\mathbf{i}}_{L_{\lambda_L}}(t) \end{pmatrix} = \begin{pmatrix} \dot{\mathbf{q}}_{C_{\gamma_G}}(t) \\ \mathbf{v}_{L_{\lambda_R}}(t) \\ \dot{\mathbf{q}}_{C_{\gamma_C}}(t) \\ \mathbf{v}_{L_{\lambda_L}}(t) \end{pmatrix}. \quad (19d)$$

With these notations, the SEs (16) become

$$\begin{pmatrix} \mathbf{M}_x \dot{\mathbf{x}}(t) \\ \mathbf{M}_y \dot{\mathbf{y}}(t) \end{pmatrix} = - \begin{pmatrix} \mathbf{H}_{11} & \mathbf{H}_{12} \\ \mathbf{H}_{21} & \mathbf{H}_{22} \end{pmatrix} \begin{pmatrix} \mathbf{x}(t) \\ \mathbf{y}(t) \end{pmatrix} - \begin{pmatrix} \mathbf{F}(\mathbf{x}(t) + \mathbf{x}_M(t_0)) \\ \mathbf{0} \end{pmatrix} - \begin{pmatrix} \mathbf{u}_x(t) \\ \mathbf{u}_y(t) \end{pmatrix} + \begin{pmatrix} \mathbf{F}(\mathbf{x}_M(t_0)) \\ \mathbf{0} \end{pmatrix} + \begin{pmatrix} \mathbf{M}_x \dot{\mathbf{x}}(t_0) \\ \mathbf{M}_y \dot{\mathbf{y}}(t_0) \end{pmatrix}.$$

This is a system of $n_C + n_L$ ODEs and the state vector in the (φ, q) -domain is $(\mathbf{x}(t), \mathbf{y}(t))^T$.

B. SEs of \mathcal{N} in the (v, i) -domain

By time-differentiation of (20) the following system of second-order ODEs are obtained (being $\dot{\mathbf{x}}(t) = \dot{\mathbf{x}}_M(t)$)

$$\begin{pmatrix} \mathbf{M}_x \ddot{\mathbf{x}}(t) \\ \mathbf{M}_y \ddot{\mathbf{y}}(t) \end{pmatrix} = - \begin{pmatrix} \mathbf{H}_{11} & \mathbf{H}_{12} \\ \mathbf{H}_{21} & \mathbf{H}_{22} \end{pmatrix} \begin{pmatrix} \dot{\mathbf{x}}(t) \\ \dot{\mathbf{y}}(t) \end{pmatrix}$$

$$- \begin{pmatrix} \mathbf{J}_F(\mathbf{x}_M(t))\dot{\mathbf{x}}(t) \\ \mathbf{0} \end{pmatrix} - \begin{pmatrix} \dot{\mathbf{u}}_x(t) \\ \dot{\mathbf{u}}_y(t) \end{pmatrix} \quad (20)$$

where $\mathbf{J}_F(\cdot) \in \mathbb{R}^{n_x \times n_x}$ is the Jacobian of $\mathbf{F}(\cdot)$ (i.e., $\mathbf{J}_F(\cdot)$ is defined by memristances and memconductances of the $n_x = n_M$ memristors). By (17), (18) and (19), these can be rewritten as a systems of SEs in the (v, i) -domain as follows

$$\dot{\mathbf{x}}_M(t) = \begin{pmatrix} \dot{\varphi}_{M_{\gamma_M}}(t) \\ \dot{\mathbf{q}}_{M_{\lambda_M}}(t) \end{pmatrix} = \begin{pmatrix} \mathbf{v}_{C_{\gamma_M}}(t) \\ \mathbf{i}_{L_{\lambda_M}}(t) \end{pmatrix} \quad (21a)$$

$$\mathbf{M}_x \begin{pmatrix} \dot{\mathbf{v}}_{C_{\gamma_M}}(t) \\ \dot{\mathbf{i}}_{L_{\lambda_M}}(t) \end{pmatrix} = -(\mathbf{H}_{11} + \mathbf{J}_F(\mathbf{x}_M(t))) \begin{pmatrix} \mathbf{v}_{C_{\gamma_M}}(t) \\ \mathbf{i}_{L_{\lambda_M}}(t) \end{pmatrix} - \mathbf{H}_{12} \begin{pmatrix} \mathbf{v}_{C_{\gamma_G}}(t) \\ \mathbf{i}_{L_{\lambda_R}}(t) \\ \mathbf{v}_{C_{\gamma_C}}(t) \\ \mathbf{i}_{L_{\lambda_L}}(t) \end{pmatrix} - \dot{\mathbf{u}}_x(t) \quad (21b)$$

$$\mathbf{M}_y \begin{pmatrix} \dot{\mathbf{v}}_{C_{\gamma_G}}(t) \\ \dot{\mathbf{i}}_{L_{\lambda_R}}(t) \\ \dot{\mathbf{v}}_{C_{\gamma_C}}(t) \\ \dot{\mathbf{i}}_{L_{\lambda_L}}(t) \end{pmatrix} = -\mathbf{H}_{21} \begin{pmatrix} \mathbf{v}_{C_{\gamma_M}}(t) \\ \mathbf{i}_{L_{\lambda_M}}(t) \end{pmatrix} - \mathbf{H}_{22} \begin{pmatrix} \mathbf{v}_{C_{\gamma_G}}(t) \\ \mathbf{i}_{L_{\lambda_R}}(t) \\ \mathbf{v}_{C_{\gamma_C}}(t) \\ \mathbf{i}_{L_{\lambda_L}}(t) \end{pmatrix} - \dot{\mathbf{u}}_y(t) \quad (21c)$$

for $t \geq t_0$. This is a system of $(n_x + n) = (n_M + n_C + n_L)$ ODEs and the state vector $\mathbf{w}(t)$ in the (v, i) -domain is

$$\begin{pmatrix} \varphi_{M_{\gamma_M}}(t) \\ \mathbf{q}_{M_{\lambda_M}}(t) \\ \mathbf{v}_{C_{\gamma_M}}(t) \\ \mathbf{i}_{L_{\lambda_M}}(t) \\ \mathbf{v}_{C_{\gamma_G}}(t) \\ \mathbf{i}_{L_{\lambda_R}}(t) \\ \mathbf{v}_{C_{\gamma_C}}(t) \\ \mathbf{i}_{L_{\lambda_L}}(t) \end{pmatrix} = \begin{pmatrix} \mathbf{x}_M(t) \\ \dot{\mathbf{x}}(t) \\ \dot{\mathbf{y}}(t) \end{pmatrix} = \mathbf{w}(t). \quad (22)$$

IV. ANALYSIS OF MANIFOLDS

As shown in the previous section, under assumptions (A1)–(A3), the large class of memristor circuits $\mathcal{N} = \mathcal{N}_{\mathcal{D}} \cup \mathcal{N}_{\mathcal{R}}$ admits of the SE representation (20) in the (φ, q) -domain. The aim is to show that from (20) we are able to investigate the existence of manifolds and the nonlinear dynamics on manifolds for such class of memristor circuits.

To this end, it is convenient to use the following change of variables in (20)

$$\mathbf{X}(t) = \mathbf{x}(t) + \mathbf{x}_M(t_0) = \mathbf{x}_M(t) \quad (23a)$$

$$\mathbf{Y}(t) = \mathbf{y}(t) - \mathbf{H}_{22}^{-1}(\mathbf{H}_{21}\mathbf{x}_M(t_0) + \mathbf{M}_y\dot{\mathbf{y}}(t_0)) \quad (23b)$$

which is well-defined under the additional assumption (named *Assumption 4*, or (A4) for short; see also Appendix A).

(A4) *Submatrix \mathbf{H}_{22} is nonsingular, i.e., $\det \mathbf{H}_{22} \neq 0$.*

It follows from (23b) that $\mathbf{Y}(t) - \mathbf{Y}(t_0) = \mathbf{y}(t) - \mathbf{y}(t_0)$ with $\mathbf{Y}(t_0) = -\mathbf{H}_{22}^{-1}(\mathbf{H}_{21}\mathbf{x}_M(t_0) + \mathbf{M}_y\dot{\mathbf{y}}(t_0))$. Hence, the change of variables (23) is also equivalent to the following

compact expressions $\mathbf{X}(t) - \mathbf{x}_M(t_0) = \mathbf{x}(t)$ and $\mathbf{Y}(t) - \mathbf{Y}(t_0) = \mathbf{y}(t)$, that permits to identify the relationship with the circuit variables given in (17).

By (23) and (20) we can derive the following form of the SEs in the (φ, q) -domain such that manifolds and the dynamics of \mathcal{N} with respect to manifolds can be grasped

$$\begin{pmatrix} \mathbf{M}_x \dot{\mathbf{X}}(t) \\ \mathbf{M}_y \dot{\mathbf{Y}}(t) \end{pmatrix} = - \begin{pmatrix} \mathbf{H}_{11} & \mathbf{H}_{12} \\ \mathbf{H}_{21} & \mathbf{H}_{22} \end{pmatrix} \begin{pmatrix} \mathbf{X}(t) \\ \mathbf{Y}(t) \end{pmatrix} - \begin{pmatrix} \mathbf{F}(\mathbf{X}(t)) \\ \mathbf{0} \end{pmatrix} - \begin{pmatrix} \mathbf{u}_x(t) \\ \mathbf{u}_y(t) \end{pmatrix} + \begin{pmatrix} \mathbf{k}_0 \\ \mathbf{0} \end{pmatrix} \quad (24)$$

where

$$\mathbf{k}_0 = \mathbf{S}_{22}\mathbf{x}_M(t_0) + \mathbf{F}(\mathbf{x}_M(t_0)) + \mathbf{M}_x\dot{\mathbf{x}}(t_0) - \mathbf{H}_{12}\mathbf{H}_{22}^{-1}\mathbf{M}_y\dot{\mathbf{y}}(t_0) \quad (25)$$

and $\mathbf{S}_{22} = \mathbf{H}/\mathbf{H}_{22} = (\mathbf{H}_{11} - \mathbf{H}_{12}\mathbf{H}_{22}^{-1}\mathbf{H}_{21})$ is the Schur complement of \mathbf{H}_{22} in \mathbf{H} . Note that $\mathbf{k}_0 \in \mathbb{R}^{n_M}$ depends upon the ICs $(\mathbf{x}_M(t_0), \dot{\mathbf{x}}(t_0), \dot{\mathbf{y}}(t_0))^T$ for the state variables in the (v, i) -domain (see equation (22)). The SEs (24) make clear that \mathbf{k}_0 plays a crucial role in the nonlinear dynamics and bifurcation phenomena of \mathcal{N} .⁸

In the following we investigate:

- *geometric properties of manifolds*, i.e., how the state space in the (v, i) -domain can be decomposed into manifolds with specific geometric properties;
- *dynamic properties of manifolds*, i.e., conditions under which the manifolds are positively invariant or not for the dynamics of \mathcal{N} in the (v, i) -domain given by the SEs (21). In the latter case the goal is to study how solutions of (21) evolve in time through different manifolds.

A. Geometric Properties

Using the expression of \mathbf{k}_0 in (25), let us introduce:

- the function $\mathbf{K}(\cdot) : \mathbb{R}^{(n_M+n_C+n_L)} \rightarrow \mathbb{R}^{n_M}$ of the state vector $\mathbf{w} = (\mathbf{x}_M, \dot{\mathbf{x}}, \dot{\mathbf{y}})$ in the (v, i) -domain⁹

$$\mathbf{K}(\mathbf{x}_M, \dot{\mathbf{x}}, \dot{\mathbf{y}}) = \mathbf{S}_{22}\mathbf{x}_M + \mathbf{F}(\mathbf{x}_M) + \mathbf{M}_x\dot{\mathbf{x}} - \mathbf{H}_{12}\mathbf{H}_{22}^{-1}\mathbf{M}_y\dot{\mathbf{y}} \quad (26)$$

- for any vector $\mathbf{k} \in \mathbb{R}^{n_M}$, the level set $\mathcal{M}(\mathbf{k}) \subset \mathbb{R}^{(n_M+n_C+n_L)}$ of $\mathbf{K}(\mathbf{x}_M, \dot{\mathbf{x}}, \dot{\mathbf{y}})$, which is defined as

$$\mathcal{M}(\mathbf{k}) = \{\mathbf{w} = (\mathbf{x}_M, \dot{\mathbf{x}}, \dot{\mathbf{y}}) \in \mathbb{R}^{n_M+n_C+n_L} : \mathbf{K}(\mathbf{w}) = \mathbf{k}\}. \quad (27)$$

Theorem 1: If (A1)–(A4) are satisfied by \mathcal{N} , then the following geometric properties hold:

- 1) for any $\mathbf{k} \in \mathbb{R}^{n_M}$, $\mathcal{M}(\mathbf{k})$ defines a nonempty, nonplanar, $(n_C + n_L)$ -dimensional manifold in the state space in the (v, i) -domain;

⁸Note that \mathbf{k}_0 depends also on circuit parameters and memristor nonlinearities (through the vector $\mathbf{F}(\cdot)$ and the submatrices of \mathbf{H} and \mathbf{M}). In this manuscript the chief interest is on the dependency on ICs in order to highlight the concept of bifurcation without parameters, whereas standard bifurcations due to the change of circuit parameters and memristor nonlinearities are not considered.

⁹In this section, the explicit time-dependency of vectors is omitted in order to highlight the geometric features of the state space in the (v, i) -domain.

- 2) for any $\mathbf{k}_1 \neq \mathbf{k}_2 \in \mathbb{R}^{n_M}$, we have $\mathcal{M}(\mathbf{k}_2) = \mathcal{M}(\mathbf{k}_1) + \mathbf{M}_x^{-1}(\mathbf{k}_2 - \mathbf{k}_1)$, i.e., $\mathcal{M}(\mathbf{k}_2)$ can be obtained via a rigid translation of $\mathcal{M}(\mathbf{k}_1)$, and conversely;
- 3) there are ∞^{n_M} nonintersecting manifolds, obtained by varying \mathbf{k} in \mathbb{R}^{n_M} , which span the whole $(n_M + n_C + n_L)$ -dimensional state space in the (v, i) -domain.

Proof: See Appendix B. ■

B. Dynamic Properties

The dynamic properties of manifolds can be inferred from the time evolution of the solutions of the SEs (21) through the $(n_M + n_C + n_L)$ -dimensional state space. Given $\mathbf{w}_0 \in \mathbb{R}^{(n_M+n_C+n_L)}$, let $\mathbf{w}(t; t_0, \mathbf{w}_0) = (\mathbf{x}_M(t), \dot{\mathbf{x}}(t), \dot{\mathbf{y}}(t))$ be the solution with ICs \mathbf{w}_0 at $t = t_0$ of the SEs (21) of \mathcal{N} in the (v, i) -domain. Using (26) and (27), if we let

$$\mathbf{k}(t; t_0, \mathbf{w}_0) = \mathbf{K}(\mathbf{w}(t; t_0, \mathbf{w}_0)), \quad \forall t \geq t_0 \quad (28)$$

then we have

$$\mathbf{w}(t; t_0, \mathbf{w}_0) \in \mathcal{M}(\mathbf{k}(t; t_0, \mathbf{w}_0)), \quad \forall t \geq t_0. \quad (29)$$

In particular, $\mathbf{w}_0 = (\mathbf{x}_M(t_0), \dot{\mathbf{x}}(t_0), \dot{\mathbf{y}}(t_0)) \in \mathcal{M}(\mathbf{k}_0)$, where $\mathbf{k}_0 = \mathbf{K}(\mathbf{x}_M(t_0), \dot{\mathbf{x}}(t_0), \dot{\mathbf{y}}(t_0))$ is given in (25).

The next property permits to study the link between the solution $\mathbf{w}(t; t_0, \mathbf{w}_0)$ at any instant $t \geq t_0$ and its associated manifold defined in (29).

Property 1: Suppose that (A1)–(A4) are satisfied by \mathcal{N} . Then, the time derivative of $\mathbf{k}(t; t_0, \mathbf{w}_0)$ in (28) is given by

$$\dot{\mathbf{k}}(t; t_0, \mathbf{w}_0) = \mathbf{H}_{12}\mathbf{H}_{22}^{-1}\dot{\mathbf{u}}_y(t) - \dot{\mathbf{u}}_x(t) \quad (30)$$

for any $\mathbf{w}_0 \in \mathbb{R}^n$ and $t \geq t_0$.

Proof: See Appendix C. ■

The expression (30) can be rewritten to highlight how we can drive solutions through different manifolds by suitable independent voltage and/or current sources

$$\begin{aligned} \dot{\mathbf{k}}(t; t_0, \mathbf{w}_0) &= \mathbf{H}_{12}\mathbf{H}_{22}^{-1}(\mathbf{B}_{21}\mathbf{e}(t) + \mathbf{B}_{22}\mathbf{a}(t)) \\ &- (\mathbf{B}_{11}\mathbf{e}(t) + \mathbf{B}_{12}\mathbf{a}(t)) \end{aligned} \quad (31)$$

from which, by integrating between t_0 and $t \geq t_0$ we have

$$\begin{aligned} \mathbf{k}(t; t_0, \mathbf{w}_0) - \mathbf{k}_0 &= \mathbf{H}_{12}\mathbf{H}_{22}^{-1}(\mathbf{B}_{21}\varphi_e(t; t_0) + \mathbf{B}_{22}\mathbf{q}_a(t; t_0)) \\ &- (\mathbf{B}_{11}\varphi_e(t; t_0) + \mathbf{B}_{12}\mathbf{q}_a(t; t_0)). \end{aligned} \quad (32)$$

The next theorem summarizes the dynamic properties of manifolds proved so far.

Theorem 2: Suppose that (A1)–(A4) are satisfied by \mathcal{N} . Then, for any $\mathbf{w}_0 \in \mathbb{R}^{(n_M+n_C+n_L)}$ we have

$$\mathbf{w}(t; t_0, \mathbf{w}_0) \in \mathcal{M}(\mathbf{k}(t; t_0, \mathbf{w}_0)), \quad \forall t \geq t_0$$

where $\mathbf{k}(t; t_0, \mathbf{w}_0)$ is a term depending on the external independent sources in \mathcal{N} given by

$$\begin{aligned} \mathbf{k}(t; t_0, \mathbf{w}_0) &= \mathbf{H}_{12}\mathbf{H}_{22}^{-1}(\mathbf{B}_{21}\varphi_e(t; t_0) + \mathbf{B}_{22}\mathbf{q}_a(t; t_0)) \\ &- (\mathbf{B}_{11}\varphi_e(t; t_0) + \mathbf{B}_{12}\mathbf{q}_a(t; t_0)) + \mathbf{k}_0 \end{aligned} \quad (33)$$

for any $t \geq t_0$, and \mathbf{k}_0 is as in (25).

Given any ICs $\mathbf{w}_0 \in \mathbb{R}^{(n_M+n_C+n_L)}$, Theorem 2 permits to find instant by instant the manifold $\mathcal{M}(\mathbf{k}(t; t_0, \mathbf{w}_0))$ containing the solution $\mathbf{w}(t; t_0, \mathbf{w}_0)$ as a linear function of the fluxes $\varphi_e(t; t_0)$, charges $\mathbf{q}_a(t; t_0)$ and parameters of $\mathcal{N}_{\mathcal{R}}$ and $\mathcal{N}_{\mathcal{D}}$.

In the next section, the r.h.s. of (31) (or equivalently (32)) is specified by voltage and/or current sources exploited in practical applications of memristor circuits.

C. Manifolds in a Relevant Class of Memristor Circuits

The results derived so far can be rewritten in a simplified form for the relevant class (see Section VI-B) of memristor circuits $\mathcal{N} = \mathcal{N}_{\mathcal{D}} \cup \mathcal{N}_{\mathcal{R}}$ having a capacitor in parallel to any flux-controlled memristor and/or an inductor in series with any charge-controlled memristor. This means that $\mathcal{N}_{\mathcal{D}}$ has only elements \mathcal{D}_M^{φ} and \mathcal{D}_M^q , i.e., $\gamma_G = \gamma_C = \lambda_R = \lambda_L = \mu_F = \mu_Q = \rho_G = \rho_R = 0$. It follows that $n_y = 0$ and that (A2), (A3) are satisfied. Note that \mathbf{H} coincides with \mathbf{H}_{11} , hence also (A4) is satisfied. In addition, $\mathbf{M}_x = \mathbf{M}$ and $\mathbf{u}_x(t) = \mathbf{u}(t) = \mathbf{B}_{11}\varphi_e(t; t_0) + \mathbf{B}_{12}\mathbf{q}_a(t; t_0)$.

If (A1) is met, the SEs in the (φ, q) -domain (24) reduce to

$$\mathbf{M}\dot{\mathbf{X}}(t) = -\mathbf{H}\mathbf{X}(t) - \mathbf{F}(\mathbf{X}(t)) - \mathbf{u}(t) + \mathbf{k}_0 \quad (34a)$$

$$\mathbf{k}_0 = \mathbf{F}(\mathbf{x}_M(t_0)) + \mathbf{M}\dot{\mathbf{x}}(t_0) + \mathbf{H}\mathbf{x}_M(t_0) \quad (34b)$$

and those in the (v, i) -domain to

$$\dot{\mathbf{x}}_M(t) = \begin{pmatrix} \dot{\varphi}_{\gamma_M}(t) \\ \dot{\mathbf{q}}_{\lambda_M}(t) \end{pmatrix} = \begin{pmatrix} \mathbf{v}_{C_{\gamma_M}}(t) \\ \mathbf{i}_{L_{\lambda_M}}(t) \end{pmatrix} \quad (35a)$$

$$\begin{aligned} \mathbf{M} \begin{pmatrix} \dot{\varphi}_{\gamma_M}(t) \\ \dot{\mathbf{i}}_{L_{\lambda_M}}(t) \end{pmatrix} &= -(\mathbf{H} + \mathbf{J}_{\mathbf{F}}(\mathbf{x}_M(t))) \begin{pmatrix} \mathbf{v}_{C_{\gamma_M}}(t) \\ \mathbf{i}_{L_{\lambda_M}}(t) \end{pmatrix} \\ &- \dot{\mathbf{u}}(t) \end{aligned} \quad (35b)$$

whereas (26) simplifies to $\mathbf{K}(\mathbf{x}_M, \dot{\mathbf{x}}) = \mathbf{H}\mathbf{x}_M + \mathbf{F}(\mathbf{x}_M) + \mathbf{M}\dot{\mathbf{x}}$ and (30) in Property 1 becomes

$$\dot{\mathbf{k}}(t; t_0, \mathbf{w}_0) = -\dot{\mathbf{u}}(t) = -(\mathbf{B}_{11}\mathbf{e}(t) + \mathbf{B}_{12}\mathbf{a}(t)) \quad (36)$$

for any $t \geq t_0$. We have $\mathbf{k}(t; t_0, \mathbf{w}_0) = -(\mathbf{B}_{11}\varphi_e(t; t_0) + \mathbf{B}_{12}\mathbf{q}_a(t; t_0)) + \mathbf{k}_0$ for any $t \geq t_0$, yielding the manifold $\mathcal{M}(\mathbf{k}(t; t_0, \mathbf{w}_0))$ as in (29) and a result analogous to Theorem 2 is obtained, then.

V. PROGRAMMING MEMRISTOR CIRCUITS WITH PULSES AND TIME-VARYING INPUTS

Theorems 1 and 2 permit to investigate the dynamic properties of autonomous and nonautonomous memristor circuits $\mathcal{N} = \mathcal{N}_{\mathcal{D}} \cup \mathcal{N}_{\mathcal{R}}$ by studying how the independent sources drive solutions $\mathbf{w}(t; t_0, \mathbf{w}_0)$ of \mathcal{N} through different manifolds in the $(n_M + n_C + n_L)$ -dimensional state space in the (v, i) -domain. In practical applications, the following main types of independent sources can be considered with regard to (31):

- memristor circuits \mathcal{N} with *no external sources*, i.e., $\mathbf{e}(t) = \mathbf{a}(t) = 0$ for any $t \geq t_0$;
- memristor circuits \mathcal{N} subject to external *pulses with finite time duration*, i.e., voltage $\mathbf{e}(t)$ and current $\mathbf{a}(t)$ sources vary over a finite time interval $[t_0, t_1]$ with $0 < t_1 - t_0 = \Delta < \infty$. The external sources are zero for any $t \geq t_1$. This class of pulses¹⁰ defines $\varphi_e(t; t_0)$ and $\mathbf{q}_a(t; t_0)$ as *sources with “constant momentum”* in the

¹⁰For simplicity, impulsive voltage and current sources instantaneously applied at t_0 can be considered by including their effects in the ICs.

(φ, q) -domain for $t \geq t_1$ (following the nomenclature introduced in [20]) and it is widely used in the experimental characterization of memristor devices and the programming of memristor-based neuromorphic systems;

- memristor circuits \mathcal{N} with voltage sources $\mathbf{e}(t)$ and/or current sources $\mathbf{a}(t)$ varying over the infinite time interval $[t_0, +\infty)$, i.e., \mathcal{N} has *sources with “time-varying momentum”* in the (φ, q) -domain. Typical examples used in several applications are:

- the class of sinusoidal voltage $\mathbf{e}(t)$ and/or current $\mathbf{a}(t)$ generators (usually considered in memristor-based filters), giving sources $\varphi_e(t; t_0)$ and $\mathbf{q}_a(t; t_0)$ with sinusoidal momentum in the (φ, q) -domain;
- the class of constant voltage $\mathbf{e}(t)$ and/or current $\mathbf{a}(t)$, providing sources $\varphi_e(t; t_0)$ and $\mathbf{q}_a(t; t_0)$ with linear time-varying momentum in the (φ, q) -domain.

A. Memristor Circuits with no External Sources

Let us consider memristor circuits $\mathcal{N} = \mathcal{N}_D \cup \mathcal{N}_R$ satisfying (A1)–(A4) with no voltage and/or current sources, that is \mathcal{N} is an *autonomous memristor* circuit with $\mathbf{e}(t) = \mathbf{a}(t) = 0$ for any $t \geq t_0$. It turns out that $\varphi_e(t; t_0) = 0$ and $\mathbf{q}_a(t; t_0) = 0$ in the (φ, q) -domain as well. Hence, $\dot{\mathbf{u}}_x(t; t_0) = 0$ and $\dot{\mathbf{u}}_y(t; t_0) = 0$ and (30) becomes $\dot{\mathbf{k}}(t; t_0, \mathbf{w}_0) = 0$ for any $\mathbf{w}_0 \in \mathbb{R}^n$ and $t \geq t_0$, i.e., $\mathbf{K}(\mathbf{x}_M, \dot{\mathbf{x}}, \dot{\mathbf{y}})$ in (26) is an *invariant of motion* for \mathcal{N} in the (v, i) -domain.

The following property summarizes the dynamics on manifolds of autonomous memristor circuits.

Property 2: Let us consider a memristor circuit \mathcal{N} with no external sources satisfying (A1)–(A4). Then, for any $\mathbf{w}_0 \in \mathbb{R}^{(n_M+n_C+n_L)}$ we have $\mathbf{w}(t; t_0, \mathbf{w}_0) \in \mathcal{M}(\mathbf{k}_0)$, $\forall t \geq t_0$, where \mathbf{k}_0 is given in (25). Moreover, the reduced-order dynamics on $\mathcal{M}(\mathbf{k}_0)$ for any $t \geq t_0$ is described in the (φ, q) -domain by the SEs (24). Finally, for any $\mathbf{k} \in \mathbb{R}^{n_M}$, the manifold $\mathcal{M}(\mathbf{k})$ defined in (27) is positively invariant for the dynamics of \mathcal{N} in the (v, i) -domain.

B. Memristor Circuits Subject to Pulses

Let us consider memristor circuits $\mathcal{N} = \mathcal{N}_D \cup \mathcal{N}_R$ satisfying (A1)–(A4) and subject to sources with constant momentum in the (φ, q) -domain for $t \geq t_1$. We have

$$\begin{aligned}\varphi_e(t; t_0) &= \varphi_e(t_1; t_0) = \int_{t_0}^{t_1} \mathbf{e}(\tau) d\tau = \bar{\mathbf{e}}\Delta, \forall t \geq t_1 \\ \mathbf{q}_a(t; t_0) &= \mathbf{q}_a(t_1; t_0) = \int_{t_0}^{t_1} \mathbf{a}(\tau) d\tau = \bar{\mathbf{a}}\Delta, \forall t \geq t_1\end{aligned}$$

where $\bar{\mathbf{e}}$ and $\bar{\mathbf{a}}$ are the mean values of $\mathbf{e}(t)$ and $\mathbf{a}(t)$ over $[t_0, t_1]$, respectively. Using these expressions, (32) becomes

$$\mathbf{k}(t_1; t_0, \mathbf{w}_0) = \mathbf{k}_1 = \mathbf{k}_0 + \mathbf{k}_u \quad (38)$$

where

$$\mathbf{k}_u = \mathbf{H}_{12}\mathbf{H}_{22}^{-1}(\mathbf{B}_{21}\bar{\mathbf{e}} + \mathbf{B}_{22}\bar{\mathbf{a}})\Delta - (\mathbf{B}_{11}\bar{\mathbf{e}} + \mathbf{B}_{12}\bar{\mathbf{a}})\Delta \quad (39)$$

takes into account the effect of the external pulses on the initial manifold $\mathcal{M}(\mathbf{k}_0)$.

Given the initial manifold $\mathcal{M}(\mathbf{k}_0)$, (38) and (39) permit to design the external pulses of $\mathbf{e}(t)$ and/or $\mathbf{a}(t)$ such that the dynamics of \mathcal{N} evolves on an assigned manifold $\mathcal{M}(\mathbf{k}_1) = \mathcal{M}(\mathbf{k}_0 + \mathbf{k}_u)$ for any $t \geq t_1$. Also note that the dynamics of \mathcal{N} is governed by the nonautonomous ODEs (24) with

$$\mathbf{u}_x(t) = \mathbf{B}_{11} \int_{t_0}^t \mathbf{e}(\tau) d\tau + \mathbf{B}_{12} \int_{t_0}^t \mathbf{a}(\tau) d\tau \quad (40a)$$

$$\mathbf{u}_y(t) = \mathbf{B}_{21} \int_{t_0}^t \mathbf{e}(\tau) d\tau + \mathbf{B}_{22} \int_{t_0}^t \mathbf{a}(\tau) d\tau \quad (40b)$$

for any $t \in [t_0, t_1]$. Point 3) in Theorem 1 ensures that the effect of $\mathbf{u}_x(t)$ and $\mathbf{u}_y(t)$ is to drive the solution $\mathbf{w}(t; t_0, \mathbf{w}_0)$ from manifold $\mathcal{M}(\mathbf{k}_0)$ to $\mathcal{M}(\mathbf{k}_1)$, i.e., for any $t \in [t_0, t_1]$ the dynamics of \mathcal{N} is continuously embedded in $\mathcal{M}(\mathbf{k}(t, t_0, \mathbf{w}_0))$ – see (28) – where $\mathcal{M}(\mathbf{k}_0)$ and $\mathcal{M}(\mathbf{k}_1)$ represent the “initial” and “final” manifolds, respectively.

The following property summarizes the dynamics on manifolds for memristor circuits subject to pulses with constant momentum for $t \geq t_1$.

Property 3: Let us consider a memristor circuit \mathcal{N} satisfying (A1)–(A4) and with constant momentum sources (37) in the (φ, q) -domain for $t \geq t_1$. Then, for any $\mathbf{w}_0 \in \mathbb{R}^{(n_M+n_C+n_L)}$ we have $\mathbf{w}(t; t_0, \mathbf{w}_0) \in \mathcal{M}(\mathbf{k}_1)$, $\forall t \geq t_1$, where $\mathbf{k}_1 = \mathbf{k}_0 + \mathbf{k}_u$, \mathbf{k}_0 is given in (25) and \mathbf{k}_u in (39) describes the effect of constant momentum sources. The reduced-order dynamics on $\mathcal{M}(\mathbf{k}_1)$ are described in the (φ, q) -domain by the SEs (24) with \mathbf{k}_0 replaced by \mathbf{k}_1 , $\mathbf{u}_x(t)$ by $(\mathbf{B}_{11}\bar{\mathbf{e}} + \mathbf{B}_{12}\bar{\mathbf{a}})\Delta$ and $\mathbf{u}_y(t)$ by $(\mathbf{B}_{21}\bar{\mathbf{e}} + \mathbf{B}_{22}\bar{\mathbf{a}})\Delta$, for any $t \geq t_1$.

Remark 2: Constant voltage and current momentum sources for $t \geq t_1$ in (37) can be obtained by means of voltage $\mathbf{e}(t)$ and/or current $\mathbf{a}(t)$ sources with *different pulse duration and amplitude*, that is, *only the area (i.e., the momentum) of the waveforms $\mathbf{e}(t)$ and/or $\mathbf{a}(t)$ over different finite time intervals is important* to set the manifold $\mathcal{M}(\mathbf{k}_1)$ on which the dynamics of \mathcal{N} takes place once all the pulses are over. This result agrees with the experimental results available in literature that show how memristors can be programmed (almost) in the same way by using triangular or squared pulses or finite impulse trains.

C. Memristor Circuits with Time-varying Sources

Let us consider memristor circuits \mathcal{N} with voltage sources $\mathbf{e}(t)$ and/or current source $\mathbf{a}(t)$ varying over the infinite time interval $[t_0, +\infty)$, i.e., \mathcal{N} has *sources with “time-varying momentum”* in the (φ, q) -domain. In this case the dynamics of \mathcal{N} for any $t \geq t_0$ is governed by the nonautonomous ODEs (24) with input $\mathbf{u}_x(t)$ and $\mathbf{u}_y(t)$ given by (40). Hence, any solution $\mathbf{w}(t; t_0, \mathbf{w}_0)$ of \mathcal{N} is embedded into the (continuous) family of manifolds parametrized by time $t \in [t_0, +\infty)$ (see (32) and Theorem 2) $\mathcal{M}(\mathbf{k}_0 + \mathbf{H}_{12}\mathbf{H}_{22}^{-1}\mathbf{u}_y(t) - \mathbf{u}_x(t))$.

Although the solution of \mathcal{N} is instant by instant on a known manifold, complex dynamic behavior and bifurcation phenomena can emerge due to the effect of the external sources with time-varying momentum in the (φ, q) -domain.

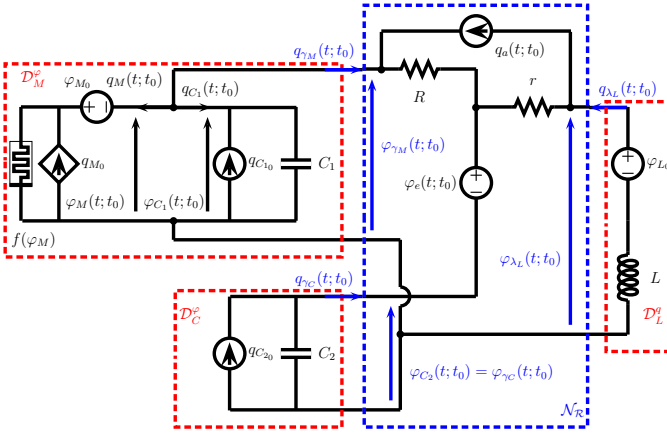


Figure 3: Memristor Chaotic Circuit (MCC) \mathcal{N} with sources $q_a(t; t_0)$ and $\varphi_e(t; t_0)$. The matrix \mathbf{H} corresponds to the hybrid representation of the three-port linear network \mathcal{N}_R connected to the elements \mathcal{D}_M^φ , \mathcal{D}_C^φ and \mathcal{D}_L^q (note that $\lambda_G = \lambda_R = 0$).

The next section presents selected examples for a thorough illustration of the explicit form of the SEs of memristor circuits $\mathcal{N} = \mathcal{N}_D \cup \mathcal{N}_R$ and their programming by tuning invariant manifolds via suitable external sources.

VI. EXAMPLES

A. Memristor Chaotic Circuit

Consider the Memristor Chaotic Circuit (MCC) \mathcal{N} obtained from that in [2, Fig. 18] by connecting sources $q_a(t; t_0)$ and $\varphi_e(t; t_0)$ as in Fig. 3. The only non-zero parameters that give the number of elements \mathcal{D}^φ and \mathcal{D}^q are: $\gamma_M = 1$, $\gamma_C = 1$ and $\lambda_L = 1$. Hence, $n_C = 2$, $n_L = 1$ and then $n_M = n_x = 1$, $n_y = 2$. A simple circuit analysis permits to prove that MCC satisfies (A1)–(A3) and derive \mathbf{H} and \mathbf{B} in (16) (being $\mathbf{G} = \mathbf{0}$ since there are no negative resistors, and $n_E = n_A = 1$)

$$\mathbf{H}_{11} = \frac{1}{R}, \quad \mathbf{H}_{12} = \begin{pmatrix} -\frac{1}{R} & 0 \end{pmatrix} = \mathbf{H}_{21}^T \quad (41a)$$

$$\mathbf{H}_{21} = \begin{pmatrix} -\frac{1}{R} \\ 0 \end{pmatrix}, \quad \mathbf{H}_{22} = \begin{pmatrix} \frac{1}{R} & -1 \\ 1 & r \end{pmatrix} \quad (41b)$$

$$\mathbf{B}_{11} = -\frac{1}{R}, \quad \mathbf{B}_{12} = -1 \quad (41c)$$

$$\mathbf{B}_{21} = \begin{pmatrix} \frac{1}{R} \\ 1 \end{pmatrix}, \quad \mathbf{B}_{22} = \begin{pmatrix} 1 \\ -r \end{pmatrix}. \quad (41d)$$

Since $\det \mathbf{H}_{22} \neq 0$, (A4) holds and MCC is described by the SEs (20) in the (φ, q) -domain where (see Fig. 3) $\mathbf{x}_M(t) = \varphi_{M\gamma_M}(t) = \varphi_{\gamma_M}(t; t_0) + \varphi_{M\gamma_M}(t_0) = \varphi_M(t)$, (with $\varphi_{M\gamma_M}(t_0) = \varphi_{M_0}$), $\mathbf{x}(t) = \varphi_{\gamma_M}(t; t_0) = \varphi_{C_1}(t; t_0)$, $\mathbf{y}(t) = (\varphi_{\gamma_C}(t; t_0), q_{\lambda_L}(t; t_0))^T = (\varphi_{C_2}(t; t_0), q_L(t; t_0))^T$,

$$u_x(t) = -\frac{1}{R}\varphi_e(t; t_0) - q_a(t; t_0) \\ = \mathbf{B}_{11}\varphi_e(t; t_0) + \mathbf{B}_{12}q_a(t; t_0) \quad (42a)$$

$$\mathbf{u}_y(t) = \begin{pmatrix} \frac{1}{R} \\ 1 \end{pmatrix} \varphi_e(t; t_0) + \begin{pmatrix} 1 \\ -r \end{pmatrix} q_a(t; t_0) \\ = \mathbf{B}_{21}\varphi_e(t; t_0) + \mathbf{B}_{22}q_a(t; t_0). \quad (42b)$$

Hence, $\mathbf{w} = (\mathbf{x}_M, \dot{\mathbf{x}}, \dot{\mathbf{y}}) = (\varphi_M, v_{C_1}, v_{C_2}, i_L)^T$ in the (v, i) -domain and function $\mathbf{K}(\varphi_M, v_{C_1}, v_{C_2}, i_L)$ and the associated manifolds $\mathcal{M}(k)$ (see (26)–(27)) are

$$\mathbf{K}(\varphi_M, v_{C_1}, v_{C_2}, i_L) = \frac{1}{r+R}\varphi_M + f(\varphi_M) \\ + C_1 v_{C_1} + \frac{rC_2}{r+R}v_{C_2} + \frac{L}{r+R}i_L \quad (43a)$$

$$\mathcal{M}(k) = \{\mathbf{w} \in \mathbb{R}^4 : \mathbf{K}(\varphi_M, v_{C_1}, v_{C_2}, i_L) = k\}, \forall k \in \mathbb{R}. \quad (43b)$$

Note that $\mathcal{M}(k)$ coincides with the expression in [2, eqs. (27)–(28)]. The 4-dimensional state space $(\varphi_M, v_{C_1}, v_{C_2}, i_L)$ in the (v, i) -domain is completely spanned by the ∞^1 3-dimensional manifolds $\mathcal{M}(k)$ by varying k in \mathbb{R} .

A simple calculation based on Property 1 and (31) yields

$$\dot{k}(t; t_0, \mathbf{w}_0) = a(t)$$

because $\mathbf{H}_{12}\mathbf{H}_{22}^{-1}\mathbf{B}_{21} = \mathbf{B}_{11}$ and $\mathbf{H}_{12}\mathbf{H}_{22}^{-1}\mathbf{B}_{22} = \mathbf{0}$. Then, the solution of the SEs (21) in the (v, i) -domain, with \mathbf{H} and \mathbf{B} in (41), and ICs $\mathbf{w}_0 = (\varphi_M(t_0), v_{C_1}(t_0), v_{C_2}(t_0), i_L(t_0))^T$

- evolves on the invariant manifold $\mathcal{M}(k_0)$ for any $t \geq t_0$, being $k_0 = \mathbf{K}(\mathbf{w}_0)$, when $q_a(t; t_0) = 0$ for any $t \geq t_0$ (cf. Property 2)
- evolves on the invariant manifold $\mathcal{M}(k_1)$ for $t \geq t_1$, being $k_1 = k_0 + \bar{a}\Delta$, when $q_a(t; t_0)$ is a constant momentum source for $t \geq t_1$ as in (37) (e.g., $q_a(t; t_0)$ in Fig. 4)
- explores the manifolds $\mathcal{M}(k_0 + a(t))$ when $q_a(t; t_0)$ is a time-varying momentum source.

The analysis makes also clear that the external source $\varphi_e(t; t_0)$ plays no role in the bifurcation phenomena of MCC. Numerical simulations confirm such qualitative analysis.

1) *Numerical simulations:* The nonlinear dynamic behavior of MCC in Fig. 3 is simulated for any $t \geq t_0 = 0$ by using the SEs (24) in the (φ, q) -domain and (42). Noting that $\mathbf{M}_x = C_1$, $\mathbf{M}_y = \text{diag}(C_2, L)$ and introducing the dimensionless variables $z_1(\tau) = X(\tau)$, $z_2(\tau) = Y_1(\tau)$, $z_3(\tau) = RY_2(\tau)$ by means of (23) (see also the derivation of (25) from (22) and Table I in [2]), the following normalized equations are derived ($n(\cdot) = Rf(\cdot)$, $R = 1 \text{ k}\Omega$, $r = 0$)

$$\frac{dz_1(\tau)}{d\tau} = \alpha[-z_1(\tau) + z_2(\tau) - n(z_1(\tau)) - w_1(\tau) + k_0] \quad (44a)$$

$$\frac{dz_2(\tau)}{d\tau} = z_1(\tau) - z_2(\tau) + z_3(\tau) - w_2(\tau) \quad (44b)$$

$$\frac{dz_3(\tau)}{d\tau} = -\beta z_2(\tau) - w_3(\tau) \quad (44c)$$

$$z_1(0) = \varphi_M(0)$$

$$z_2(0) = -Li_L(0)$$

$$z_3(0) = -\varphi_M(0) + C_2 v_{C_2}(0) - Li_L(0)$$

where $w_1(\tau) = -\varphi_e(\tau; \tau_0) - q_a(\tau; \tau_0) = -w_2(\tau)$, $w_3(\tau) = \varphi_e(\tau; \tau_0)$, $\mathbf{Y}(0) = -\mathbf{H}_{22}^{-1}(\mathbf{H}_{21}\varphi_M(0) + \mathbf{M}_y\dot{\mathbf{y}}(0))$, the CR of the memristor is $n(z_1) = -m_0 z_1 + m_1 z_1^3$ with $m_0 = 8/7$ and $m_1 = 4/63$, $\tau = t/(RC_2)$ is the normalized time (in $[\mu\text{s}]$), $\alpha = C_2/C_1$, $\beta = (R^2 C_2)/L = C_2/L$.

Let us consider $\varphi_e(\tau; \tau_0) = 0$ (i.e., $w_3(\tau) = 0, \forall \tau \geq 0$) and the constant momentum source $u_x(\tau) = -q_a(\tau; 0) = w_1(\tau)$ (cf. (42)) shown in Fig. 4, which is defined by rectangular pulses $a(\tau)$ with finite time duration $\Delta = 10$ and amplitude $A \neq 0$ between the instants $T_0 = 300$ and $T_1 = T_0 + \Delta = 310$ (normalized time units). Given the ICs in the (v, i) -domain $\mathbf{w}_0 = (\varphi_M(0), v_{C_1}(0), v_{C_2}(0), i_L(0))^T$, the SEs (44) describe the dynamics of MCC on the manifold $\mathcal{M}(k_0)$ with $k_0 = \varphi_M(0) + n(\varphi_M(0)) + C_1 v_{C_1}(0) + Li_L(0)$ (see (25) with the normalized values $R = 1$ and $r = 0$) as long as the constant momentum source $q_a(\tau; 0)$ is zero, i.e., for all $\tau \in [0, T_0]$. As shown in [2, Fig. 21(a)], MCC exhibits a double-scroll when the ICs \mathbf{w}_0 are such that $k_0 = 0$. Let us assume $k_0 = 0$ and show that the nonlinear dynamics of MCC can be programmed by means of suitable pulses $a(\cdot)$ with finite time duration as those in Fig. 4. Due to the pulse, the dynamics evolves from the manifold $\mathcal{M}(k_0)$ onto a different manifold $\mathcal{M}(k_1)$ for $\tau > T_1$, where k_1 is given by (38), i.e., $k_1 = k_u = A\Delta$. Suppose we first choose $A = -0.00281$. In this case it is apparent that the dynamics for $\tau > T_1$ on the manifold $\mathcal{M}(-0.0281)$ results to be the spiral chaotic attractor shown in [2, Fig. 21(c)]. Fig. 5 shows how the pulse with $A = -0.00281$ in Fig. 4 induces a bifurcation of the chaotic attractor in MCC of Fig. 3 with *fixed circuit parameters* $\alpha = 9.5$ and $\beta = 15$. Such results are also shown in Fig. 5b where the whole waveforms of $X(\tau)$, $Y_1(\tau)$ and $Y_2(\tau)$ are reported for $\tau \in [0, 1000]$. It is seen that the double-scroll chaotic attractor (blue curve) for $k_0 = 0$ (i.e., for $0 \leq \tau \leq T_0$) turns into a spiral chaotic attractor (green curve) for $k_1 = -0.0281$ (i.e., for $\tau \geq T_1$). When the pulse in Fig. 4 is applied (i.e., $T_0 \leq \tau \leq T_1$) the dynamics (red curve in Fig. 5a) evolves from the manifold $\mathcal{M}(k_0 = 0)$ to $\mathcal{M}(k_1 = 0.0281)$, i.e., from the double-scroll to the spiral chaotic attractor. Similar results have been obtained if the rectangular pulses in Fig. 4 are replaced by triangular pulses or pulses with arbitrary waveforms, provided their charge momentum is equal to -0.0281 .

Fig. 6 shows how the pulse with $A = 0.00781$ in Fig. 4 induces a different bifurcation. With reference to Fig. 6, the blue curve is the dynamics for $0 \leq \tau \leq 300$, (i.e., when the pulse has not yet been applied), the red curve is the dynamics for $300 \leq \tau \leq 310$ (i.e., when the pulse is applied) and the green curve is the dynamics for $\tau \geq 310$ (i.e., when the pulse is over). It is apparent that in this case the double-scroll chaotic attractor turns into a period-three limit cycle (black curve in Fig. 6) due to the pulse.

Several other *Pulse-Induced Bifurcations* (PiB) have been observed in other memristor circuits $\mathcal{N} = \mathcal{N}_{\mathcal{R}} \cup \mathcal{N}_{\mathcal{D}}$ (simulations are not reported here for the lack of space). Such numerical simulations allow us to draw the important conclusion that the nonlinear dynamics of memristor circuits can be programmed via pulse with finite time duration (i.e., constant momentum sources in the (φ, q) -domain) and the *analysis through manifolds in the (φ, q) -domain permits to effectively design the required pulse parameters* (i.e., duration and amplitude).

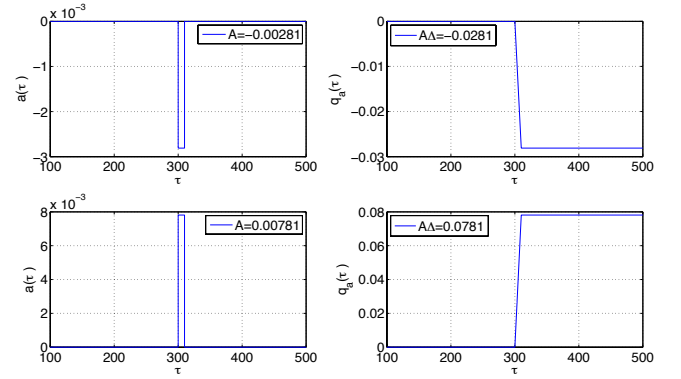


Figure 4: The current source $a(t)$ is a rectangular pulse with finite time duration such that $q_a(t; t_0)$ in Fig. 3 represents a constant momentum source. The pulses have amplitude $A \neq 0$ only between $T_0 = 300$ and $T_1 = 310$ (i.e., $\Delta = 10$ in normalized time units); we have $A = -0.00281$ (upper part) and $A = 0.00781$ (bottom part).

B. Memristor Star-CNNs

In this short section we discuss potential applications of the flux-charge analysis method and pulse programming of nonlinear dynamics on manifolds in large memristor circuits.

Let us consider neural networks with a star topology and a large number N of cells, where each cell is represented by an element \mathcal{D}^φ with a capacitor and a flux-controlled memristor in parallel. Neural networks with a star topology are also referred to as Star-CNNs ([25], [26]). Hereinafter, the studied Star-CNNs with memristors are named Memristor Star-CNNs (MS-CNNs). It is apparent that MS-CNNs fall into the class of memristor circuits described in Section IV-C. To simplify the notation, time is not explicitly reported, we let $t_0 = 0$ and denote $\varphi_{\gamma_M}^{(i)} = \varphi_i$, $q_{\gamma_M}^{(i)} = q_i$, $\varphi_M^{(i)}(0) = \varphi_{M_{0_i}}$ and $G = \sum_{j=1}^N G_j$ (see Fig. 7). The vectors of fluxes $\boldsymbol{\varphi} = (\varphi_1, \dots, \varphi_N)^T$, charges $\mathbf{q} = (q_1, \dots, q_N)^T$, $\boldsymbol{\varphi}_{M_0} = (\varphi_{M_{0_1}}, \dots, \varphi_{M_{0_N}})^T$ and $\boldsymbol{\varphi}_e = (\varphi_{e_1}, \dots, \varphi_{e_N})^T$ permit to write via Millmann's theorem the SEs of MS-CNNs in the (φ, q) -domain in the compact form (see also (34))

$$\mathbf{M}\dot{\boldsymbol{\varphi}} = -\mathbf{H}\boldsymbol{\varphi} - F(\boldsymbol{\varphi} + \boldsymbol{\varphi}_{M_0}) + \mathbf{k}_0 - \mathbf{u} \quad (45a)$$

$$\mathbf{k}_0 = F(\boldsymbol{\varphi}_{M_0}) + \mathbf{M}\dot{\boldsymbol{\varphi}}_{M_0} + \mathbf{H}\boldsymbol{\varphi}_{M_0} \quad (45b)$$

$$\boldsymbol{\varphi}(0) = \boldsymbol{\varphi}_{M_0}$$

where $\mathbf{u} = \mathbf{H}\boldsymbol{\varphi}_e + \mathbf{B}_{12}q_a$, the entry (i, j) of \mathbf{B}_{11} (for $1 \leq i \leq N$ and $1 \leq j \leq N$) is $[\mathbf{B}_{11}]_{ij} = -G_i G_j / G$, $\mathbf{H} = \text{diag}(G_1, \dots, G_N) + \mathbf{B}_{11}$, $\mathbf{B}_{12} = (-G_1/G, \dots, -G_N/G)^T$ and $\mathbf{M} = \text{diag}(C_1, \dots, C_N)$.

If \mathbf{u} is constant, the *number and stability properties of equilibrium points* in the MS-CNNs described by (45) depend on \mathbf{k}_0 and \mathbf{u} . In particular, bifurcations of such equilibria can be induced by applying pulses with finite time duration by means of $\boldsymbol{\varphi}_e$ and q_a , which cause a change of \mathbf{k}_0 into $\mathbf{k}_0 + \mathbf{k}_u$ with \mathbf{k}_u given in (39). No further analysis is presented for the lack of space. A detailed investigation of MS-CNNs will be reported in a further work.

VII. CONCLUSION

The paper has provided an explicit general form for the SEs of a broad class of memristor circuits with an arbitrary

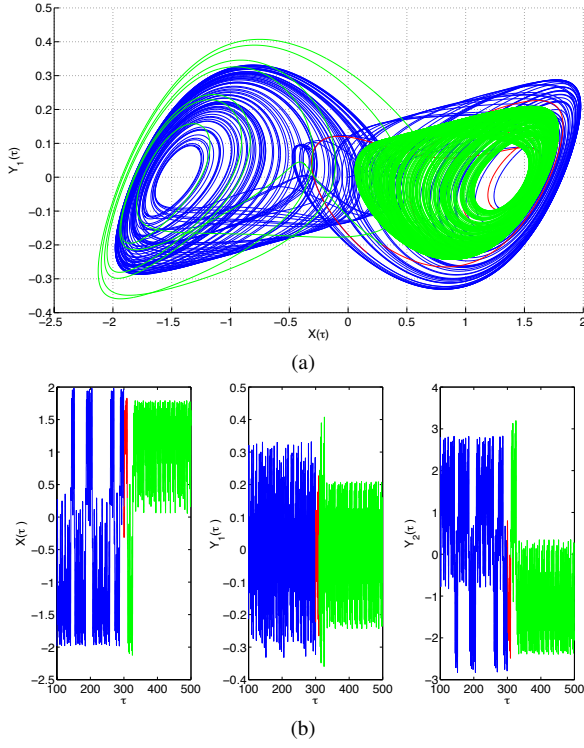


Figure 5: Pulse-induced Bifurcations of the chaotic attractor in MCC of Fig. 3 with fixed circuit parameters $\alpha = 9.5$ and $\beta = 15$. The double-scroll chaotic attractor (blue curve) for $k_0 = 0$ (i.e., for $0 \leq \tau \leq T_0$) turns into a spiral chaotic attractor (green curve) for $k_1 = -0.0281$ (i.e., for $\tau \geq T_1$). When the pulse in Fig. 4 is applied (i.e., $T_0 \leq \tau \leq T_1$) the dynamics (red curve) evolves from manifold $\mathcal{M}(k_0 = 0)$ to manifold $\mathcal{M}(k_1 = 0.0281)$, i.e., from the manifold with a double-scroll chaotic attractor to a manifold with a spiral chaotic attractor.

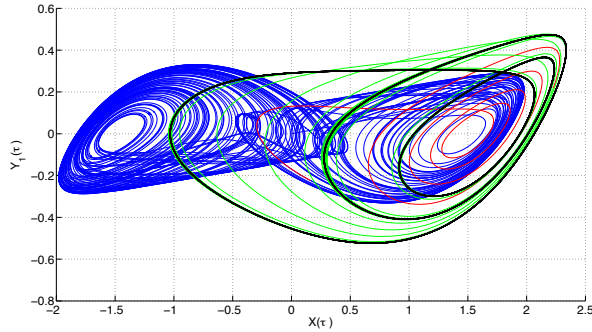


Figure 6: Bifurcation induced by the pulse in Fig. 4 with $A = 0.00781$. The double-scroll chaotic attractor turns into a period-three limit cycle. The black curve represents the period-three limit cycle when $\tau \in [900, 1000]$.

number of inductors, capacitors and flux- or charge-controlled memristors. In the spirit of [21], conditions for the existence of the SEs are couched in graph-theoretic terms and as such they can be checked by inspection on the circuit topology. On the basis of the SEs it is shown that the state space in the (v, i) -domain can be decomposed in infinitely many manifolds and that, in the autonomous case, each manifold is positively invariant for the dynamics and is characterized by a reduced-order dynamics and attractors in the (φ, q) -domain. The chief

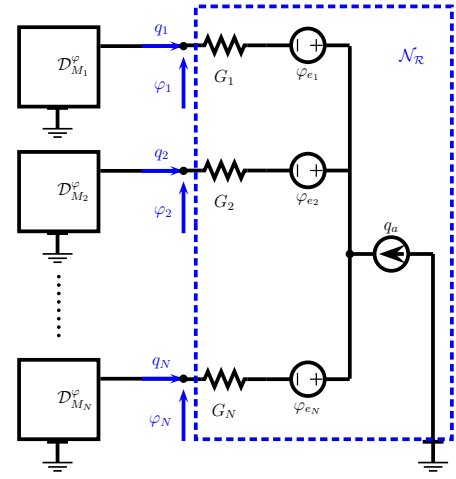


Figure 7: Memristor Star-CNNs. Each cell is represented by an element \mathcal{D}_M^φ with a capacitor and a flux-controlled memristor in parallel. The matrix \mathbf{H} corresponds to the hybrid representation of the N -port linear network \mathcal{N}_R .

results in the paper concern the non-autonomous case where time-varying independent sources are present. In such a case, general explicit formulas are obtained for designing pulses with finite time-duration in order to program the different nonlinear dynamics that can be displayed by the memristor circuits, i.e., to drive at one will solutions between different manifolds, reduced dynamics and attractors. This gives a sound theoretical foundation to a common practice for changing the dynamics in memristor circuits that has been so far mainly based on experimental trials and/or heuristic means.

APPENDIX A NONSINGULARITY OF \mathbf{H}_{22}

We provide some brief considerations about assumption (A4). Consider for simplicity a network \mathcal{N} satisfying (A1)–(A3) with only one flux-controlled memristor M in parallel to C_1 . Also suppose that \mathcal{N} has only positive resistors, i.e., $\gamma_G = \lambda_R = \rho_G = \rho_R = 0$. In this case, we can show that (A4) is satisfied, i.e., $\det \mathbf{H}_{22} \neq 0$, if and only if the next topological assumption holds.

(A5) *The network \mathcal{N} has no cutsets made of capacitors C_2, \dots, C_{n_C} and/or charge sources and no loops made of M , inductors L_1, \dots, L_{n_L} and/or flux sources.*

The proof, which is omitted due to space limitations, follows by an argument for testing the nonsingularity of the hybrid representation of \mathcal{N}_R as in Corollary 3 in [24].¹¹ Furthermore, if (A4) fails, then the state space in the (v, i) -domain can be decomposed in ∞^1 planar manifolds. To see this, note that, since also (A5) fails, there exists for instance a loop made by M, L_1, \dots, L_{n_L} and/or flux sources. Suppose the loop is made by M, L_1, L_2 and a flux source $\varphi_e(t)$. Assuming a positive sign before each voltage term, the Kirchhoff Voltage Law yields $d(\varphi_M(t) + L_1 i_{L_1}(t) + L_2 i_{L_2}(t))/dt = -e(t)$ for

¹¹For example, it can be verified that the memristor chaotic circuit in Fig. 3 satisfies (A5), and indeed we have explicitly seen that $\det \mathbf{H}_{22} \neq 0$.

any $t \geq t_0$. Then, we can identify ∞^1 manifolds $\mathcal{M}(k) = \{(\varphi_M, v_{C_1}, \dots, v_{C_{n_C}}, i_{L_1}, \dots, i_{L_{n_L}})^T \in \mathbb{R}^{n_C+n_L+1} : \varphi_M + L_1 i_{L_1} + L_2 i_{L_2} = k\}$, $k \in \mathbb{R}$, spanning the state space, with properties analogous to those found in Sections IV and V. Each manifold is an $(n_C + n_L)$ -dimensional plane.

In the more general case where \mathcal{N} has also negative resistors, we have been able so far to obtain only some preliminary results. For example, it can be seen that (A5) is a necessary but not sufficient condition for (A4). Also in this case, when (A4) fails, it is possible to prove via algebraic arguments the existence of ∞^1 planar manifolds into which the state space in the (v, i) -domain can be decomposed. However, it seems difficult to find such manifolds via topological arguments.

APPENDIX B PROOF OF THEOREM 1

- 1) Given any $\mathbf{k} \in \mathbb{R}^{n_M}$, it can be easily checked that $\mathcal{M}(\mathbf{k})$ contains at least the point $\mathbf{w} = (0, \mathbf{M}_x^{-1}(\mathbf{k} - \mathbf{F}(0)), 0)$, hence $\mathcal{M}(\mathbf{k}) \neq \emptyset$. The manifold $\mathcal{M}(\mathbf{k})$ is non-planar due to the nonlinear function $\mathbf{F}(\cdot)$. Finally, function $\mathbf{K}(\mathbf{w}) = \mathbf{k}$ specifies n_M constraints in the $(n_M + n_C + n_L)$ -dimensional state space in the (v, i) -domain. Hence, the dimension of $\mathcal{M}(\mathbf{k})$ is given by $(n_C + n_L)$ independent state variables in the (v, i) -domain.
- 2) Consider the following class of rigid translations: $\mathbf{x}_M \rightarrow \mathbf{x}_M + \Delta\mathbf{x}$, $\dot{\mathbf{x}} \rightarrow \dot{\mathbf{x}} + \Delta\dot{\mathbf{x}}$, $\dot{\mathbf{y}} \rightarrow \dot{\mathbf{y}} + \Delta\dot{\mathbf{y}}$. Also consider the equation $\mathbf{M}_x \Delta\dot{\mathbf{x}} - \mathbf{H}_{12} \mathbf{H}_{22}^{-1} \mathbf{M}_y \Delta\dot{\mathbf{y}} = \mathbf{k}_2 - \mathbf{k}_1$, that has a solution $\Delta\dot{\mathbf{x}} = \mathbf{M}_x^{-1}(\mathbf{k}_2 - \mathbf{k}_1)$, $\Delta\dot{\mathbf{y}} = 0$ and possibly other solutions. We have $\mathbf{K}(\mathbf{w} + (0, \Delta\dot{\mathbf{x}}, 0)) = \mathbf{K}(\mathbf{w}) + \mathbf{k}_2 - \mathbf{k}_1$. This means that, for any $\mathbf{w} \in \mathcal{M}(\mathbf{k}_1)$, we have $\mathbf{w} + (0, \Delta\dot{\mathbf{x}}, 0) \in \mathcal{M}(\mathbf{k}_2)$. Conversely, for any $\mathbf{w} \in \mathcal{M}(\mathbf{k}_2)$ we have $\mathbf{w} - (0, \Delta\dot{\mathbf{x}}, 0) \in \mathcal{M}(\mathbf{k}_1)$.
- 3) Manifolds are nonintersecting because if there exist $\mathbf{w} \in \mathcal{M}(\mathbf{k}_1) \cap \mathcal{M}(\mathbf{k}_2)$, with $\mathbf{k}_1 \neq \mathbf{k}_2$, then $\mathbf{K}(\mathbf{w}) = \mathbf{k}_1$ and $\mathbf{K}(\mathbf{w}) = \mathbf{k}_2$, i.e., \mathbf{w} is mapped by $\mathbf{K}(\cdot)$ in two distinct vectors \mathbf{k}_1 and \mathbf{k}_2 , while $\mathbf{K}(\cdot)$ in (26) is a (single-valued) function. Since manifolds are parametrized by the n_M -dimensional vector \mathbf{k} , we conclude that there are ∞^{n_M} nonintersecting manifolds. To see that they fill the whole state space, it is enough to note that, given any point \mathbf{w} , we have $\mathbf{w} \in \mathcal{M}(\mathbf{K}(\mathbf{w}))$.

APPENDIX C PROOF OF PROPERTY 1

Due to (26), being $\dot{\mathbf{x}}_M(t) = \dot{\mathbf{x}}(t)$, we have $\dot{\mathbf{k}}(t; t_0, \mathbf{w}_0) = \mathbf{S}_{22}\dot{\mathbf{x}}(t) + \mathbf{J}_F(\mathbf{x}_M(t))\dot{\mathbf{x}}(t) + \mathbf{M}_x\dot{\mathbf{x}}(t) - \mathbf{H}_{12}\mathbf{H}_{22}^{-1}\mathbf{M}_y\dot{\mathbf{y}}(t)$. Using such equation, the expression in (30) is easily obtained by the following relationships derived from (21)

$$\begin{aligned} \mathbf{J}_F(\mathbf{x}_M(t))\dot{\mathbf{x}}(t) + \mathbf{M}_x\dot{\mathbf{x}}(t) &= -\mathbf{H}_{11}\dot{\mathbf{x}}(t) - \mathbf{H}_{12}\dot{\mathbf{y}}(t) - \dot{\mathbf{u}}_x(t) \\ \mathbf{M}_y\dot{\mathbf{y}}(t) &= -\mathbf{H}_{21}\dot{\mathbf{x}}(t) - \mathbf{H}_{22}\dot{\mathbf{y}}(t) - \dot{\mathbf{u}}_y(t). \end{aligned}$$

REFERENCES

- [1] F. Corinto and M. Forti, "Memristor circuits: Flux-charge analysis method," *IEEE Trans. Circuits Syst. I, Reg. Papers*, vol. 63, no. 11, pp. 1997–2009, Nov. 2016, DOI: 10.1109/TCSI.2016.2590948.
- [2] —, "Memristor circuits: Bifurcations without parameters," *IEEE Trans. Circuits Syst. I, Reg. Papers*, vol. 64, 2017, published online. DOI: 10.1109/TCSI.2016.2642112.

- [3] M. Itoh and L. O. Chua, "Memristor oscillators," *Int. J. Bifurcation Chaos*, vol. 18, no. 11, pp. 3183–3206, 2008.
- [4] R. Riaza and C. Tischendorf, "Semistate models of electrical circuits including memristors," *Int. J. Circuit Theory Appl.*, vol. 39, no. 6, pp. 607–627, 2011.
- [5] A. Ascoli, R. Tetzlaff, L. O. Chua, J. P. Strachan, and R. S. Williams, "History erase effect in a non-volatile memristor," *IEEE Trans. Circuits Syst. I: Reg. Papers*, vol. 63, no. 3, pp. 389–400, 2016.
- [6] A. Ascoli, F. Corinto, and R. Tetzlaff, "Generalized boundary condition memristor model," *Int. J. Circuit Theory Appl.*, vol. 44, no. 1, pp. 60–84, 2016.
- [7] A. Ascoli, S. Slesazeck, H. Mähne, R. Tetzlaff, and T. Mikolajick, "Non-linear dynamics of a locally-active memristor," *IEEE Trans. Circuits Syst. I: Reg. Papers*, vol. 62, no. 4, pp. 1165–1174, 2015.
- [8] J. Secco, F. Corinto, and A. Sebastian, "Flux-charge memristor model for phase change memory," *IEEE Trans. Circuits Syst. II: Expr. Briefs*, 2017.
- [9] M. Orlowski, J. Secco, and F. Corinto, "Chua's constitutive memristor relations for physical phenomena at metal-oxide interfaces," *IEEE J. Emerg. Selec. Topics Circuits Syst.*, vol. 5, no. 2, pp. 143–152, 2015.
- [10] F. Corinto, P. P. Civalleri, and L. O. Chua, "A theoretical approach to memristor devices," *IEEE J. Emerg. Selec. Topics Circuits Syst.*, vol. 5, no. 2, pp. 123–132, 2015.
- [11] J. Ma, F. Wu, G. Ren, and J. Tang, "A class of initials-dependent dynamical systems," *Appl. Math. Comput.*, vol. 298, pp. 65–76, 2017.
- [12] B. Bao, N. Wang, Q. Xu, H. Wu, and Y. Hu, "A simple third-order memristive band pass filter chaotic circuit," *IEEE Trans. Circuits Syst. II: Expr. Briefs*, 2016, published online. DOI:10.1109/TCSI.2016.2641008.
- [13] B. Bao, T. Jiang, Q. Xu, M. Chen, H. Wu, and Y. Hu, "Coexisting infinitely many attractors in active band-pass filter-based memristive circuit," *Nonlinear Dynamics*, vol. 86, no. 3, pp. 1711–1723, 2016.
- [14] A. Buscarino, C. Corradino, L. Fortuna, M. Frasca, and L. O. Chua, "Turing patterns in memristive cellular nonlinear networks," *IEEE Trans. Circuits Syst. I: Reg. Papers*, vol. 63, no. 8, pp. 1222–1230, 2016.
- [15] V.-T. Pham, S. Vaidyanathan, C. Volos, S. Jafari, N. Kuznetsov, and T. Hoang, "A novel memristive time-delay chaotic system without equilibrium points," *Eur. Phys. J.: Spec. Topics*, vol. 225, no. 1, pp. 127–136, 2016.
- [16] R. Riaza, "Manifolds of equilibria and bifurcations without parameters in memristive circuits," *SIAM J. Appl. Math.*, vol. 72, no. 3, pp. 877–896, 2012.
- [17] B. Bao, Z. Ma, J. Xu, Z. Liu, and Q. Xu, "A simple memristor chaotic circuit with complex dynamics," *Int. J. Bifurc. Chaos*, vol. 21, no. 9, pp. 2629–2645, 2011.
- [18] Q. Li, S. Hu, S. Tang, and G. Zeng, "Hyperchaos and horseshoe in a 4D memristive system with a line of equilibria and its implementation," *Int. J. Circuit Theory Appl.*, vol. 42, no. 11, pp. 1172–1188, 2014.
- [19] F. Corinto, A. Ascoli, and M. Gilli, "Analysis of current-voltage characteristics for memristive elements in pattern recognition systems," *Int. J. Circuit Theory Appl.*, vol. 40, no. 12, pp. 1277–1320, Dec. 2012.
- [20] F. Corinto, P. P. Civalleri, and L. O. Chua, "A theoretical approach to memristor devices," *IEEE J. Emerg. Select. Topics Circuits Syst.*, vol. 5, no. 2, pp. 123–132, 2015.
- [21] L. O. Chua, "Dynamic nonlinear networks: state-of-the-art," *IEEE Trans. Circuits Syst.*, vol. 27, no. 11, pp. 1059–1087, 1980.
- [22] M. Hasler, "State equations for active circuits with memristors," in *Chaos, CNN, Memristors and Beyond: A Festschrift for Leon Chua*. World Scientific, 2013, pp. 518–528.
- [23] W. K. Chen, *Applied graph theory*. Netherlands: North-Holland, 1976.
- [24] H. C. So, "On the hybrid description of a linear n -port resulting from the extraction of arbitrarily specified elements," *IEEE Trans. Circuit Theory*, vol. CT-12, no. 3, pp. 381–387, 1965.
- [25] M. Itoh and L. O. Chua, "Star cellular neural networks for associative and dynamic memories," *Int. J. Bifurc. Chaos*, vol. 14, no. 05, pp. 1725–1772, 2004.
- [26] F. Corinto, M. Gilli, and T. Roska, "On full-connectivity properties of locally connected oscillatory networks," *IEEE Trans. Circuits Syst. I: Reg. Papers*, vol. 58, no. 5, pp. 1063–1075, 2011.
- [27] L. O. Chua, "Memristor-The missing circuit element," *IEEE Trans. Circuit Theory*, vol. 18, no. 5, pp. 507–519, 1971.